An Alternative Method to Access Diverse N,N′-Diquaternised-3,3′-biquinoxalinium "Biquinoxen" Dications†

Nicolas Leblanc,[a] Stephen Sproules,[b] and Annie Powell*[a,c]*

[a]Institut für Nanotechnologie, Karlsruher Institut für Technologie, Harmann-von-Helmholtz-Platz 1, D-76344 Eggenstein-Leopoldshafen, Germany, [b]WestCHEM, School of Chemistry, University pof Glasgow, Glasgow G12 8QQ, U.K., and [c]Institut für Anorganische Chemie, Karlsruher Institut für Technologie, Eggenstraße 15, D-76131 Karlsruhe, Germany

E-mail: nicolas.leblanc@partner.kit.edu; annie.powell@kit.edu

Abstract. An alternative synthetic route for the design of *N*,*N*′-diquaternised-3,3′-biquinoxalinium "biquinoxen" dications is reported, involving oxidative radical coupling of dithionite reduced quinoxaline quaternary salts. Although the reaction is not regioselective, leading to relatively modest yields (up to 32%), the advantages of this new synthetic protocol lie in a simple potentially gram scale synthesis using inexpensive easily accessible reagents with no metal catalysts and no purification steps. Thus whereas the method reported previously to access the *N*,*N*′-dimethyl-3,3′-biquinoxalinium, "methylbiquinoxen" precursor gave higher yield than the new method reported here, this new method avoids the limitation of using scarce oxonium reagents. Overall, the new protocol is a robust synthetic strategy which offers new design possibilities.

Introduction

Combining the redox activity of viologens[1] in concert with the chelating function of a simple organic ligand such as 2,2′-bipyridine is an important challenge since it would provide a unique opportunity to create robust metal/ligand complexes with exotic and tuneable electronic structures. This would produce strongly correlated phenomena between the ligand and any metalloid centre with potential applications such as in spin labelling, catalysis or molecular magnetism.

In this context, since the pioneering work of Kaim on 3,3′-bipyrazinium and 4,4′-bipyrimidinium based chelates and their studies as spin labels,[2-4] we reported a new multifunctional chelating organic ligand, the *N,N*′-dimethyl-3,3′-biquinoxalinium "methylbiquinoxen" dication, (**Mbqn^{2+}**), the first member of a new family of 3,3′-biquinoxalinium diquaternary salts coined "biquinoxens" (Fig. 1). Surprisingly, such a simple and stable pro-ligand revealed a promising versatility. Indeed the **Mbqn^{2+}** platform proved not only to combine a rich redox and Lewis acid/base chemistry combined with the chelating functionality, but also shows tuneable luminescence as well as providing the possibility of covalent functionalisation similar to the "click" chemistry approach.[5,6]

Furthermore, besides being simple to synthesise in a pure form, in good yield and gram quantities in as little as two steps, the multiple properties are anchored on the same 1,4-diazine core structure of the **Mbqn^{2+}** which offers exciting prospects for the design of organic or hybrid organic-inorganic based molecular compounds with interconnected and synchronous properties.

In terms of the synthesis, the diquaternisation of biquinoxaline[7] using Meerwein alkylation was found to be the easiest way to obtain **Mbqn^{2+}** (Fig. 1). However, extension of this method to target other diquaternised biquinoxens is clearly limited due to the poor nucleophilicity of biquinoxaline, substantiated by the fact that very few biquinoxaline-based coordination complexes have been reported and mostly use diamagnetic metal ions.[8,9] Thus, although using oxonium derivatives as a last resort proved to be a remarkably successful pathway to target the desired **Mbqn^{2+}**, such strong alkylating agents are scarce and mostly not commercially available. This significantly hinders current access to the

synthesis of further members of this family using the left hand route in figure 1 and therefore we explored an alternative route.

In the context of the potential of biquinoxens derivatives and the challenges to be addressed, we report here a novel route to design *N,N′*-diquaternised biquinoxens, which instead of using biquinoxaline involves the oxidative radical coupling of chemically reduced quinoxaline quaternary salts (Fig. 1).

Following this new method, joining the broad family of oxidative radical cross-coupling reactions,[10] we have been able to reproduce the Mbqn precursor and to get three new homologues, namely ethylbiquinoxen (**Ebqn**$^{2+}$), propylbiquinoxen (**Pbqn**$^{2+}$) and benzylbiquinoxen (**Bzbqn**$^{2+}$). Since the chemistry of quinoxaline quaternary salts is well-known but demanding in terms of synthesis,[11] the purpose of this paper is to introduce this alternative method rather than presenting the whole library of biquinoxens which can be synthesised in this way.

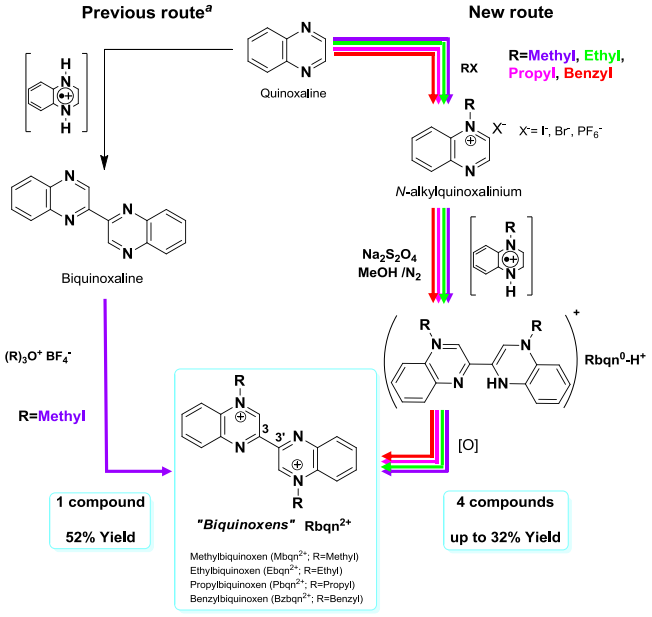

Fig. 1 Previous route (left path) as reported and discussed in *a* = ref 5 for the synthesis of the methylbiquinoxen Mbqn^{2+} only. Alternative and more versatile (right path) synthetic route for the design of various *N,N′*-disubstituted-3,3′-biquinoxalinium "Biquinoxens" Rbqn^{2+} with R = methyl, ethyl, propyl and benzyl.

Results and Discussion

Synthetic Procedures. Compounds **Rbqn^{2+}** (R= M (methyl), E (ethyl), P (propyl), Bz (benzyl)) were obtained according to the following general procedure (see ESI for synthetic details of all compounds).

A Schlenk was charged with the corresponding *N*-monoquaternised quinoxalinium cation [RQ](X) (X^- = I, Br, PF_6) and an excess of sodium dithionite ($Na_2S_2O_4$) in MeOH. The system was purged with nitrogen, closed and agitated in an ultrasound bath for 15 min. Upon standing for 7 d, a purple microcrystalline solid had formed from the dark blue reaction mixture. This was isolated by filtration, copiously-washed with MeOH and water, then dried under vacuum. Electronic and IR spectroscopy as well as elemental analysis have been performed on each samples. Complementary single crystal X-ray diffraction analysis has been also performed only in the case of R = propyl. All the experiments confirm that the purple products correspond to the direduced monoprotonated cationic form **Rbqn^0-H$^+$** (Fig. 1) of the corresponding biquinoxen dications **Rbqn^{2+}**, as already known for **Mbqn^0-H$^+$**.[5] Furthermore, the presence of sulfur in each elemental analysis (ESI) shows that the charge of the organic moieties is at least always partially balanced by some sulfur oxygen containing anions.

In particular, the purple powders exhibit a characteristic broad absorption in the range 200–1400 nm as well as strong IR vibrations in the 1580–1720 cm^{-1} region (ESI). In all cases these optical and vibrational signatures are in line with the one obtained by studying crystals of **MBqn^0-H$^+$**[BF_4] for which the protonation has been perfectly proved.[5] However, we notice an increase of the IR vibration peak from 1638 to 1695 cm^{-1} as the bulkiness, and probably the twist angle around the central C–C bond, of the R substituent increases from methyl to benzyl (ESI).

In order to confirm that the purple intermediates correspond to the direduced monoprotonated species **Rbqn^0-H$^+$** a complementary X-ray structure determination has been performed on dark purple crystals in the case of R = propyl and is consistent with the formula [**Pbqn^0-H$^+$**]$_2$($S_4O_6^{2-}$), the **Pbqn^0-H$^+$** species being balanced here by the presence of tetrathionate ion. Although the dataset is reliable, the very small

size of the crystal precluded definitive identification of all the H-atoms from Fourier difference maps. However the structure analysis revealed the features characteristic of a direduced monoprotonated species (Figure 2), as it has been unambiguously described for **Mbqn^0-H$^+$**.[5] In particular, the two crystallographically independent **Pbqn^0-H$^+$** units adopt the typical *cis*-configuration (φ = 7.2° and 8.3°) where the dihedral angle is defined as $\varphi = C_2–C_3–C_3'–C_2'$. Remarkably, compared with **Mbqn^0-H$^+$** (φ = 2.5),[5] the larger dihedral angles for **Pbqn^0-H$^+$** confirm that the increase of the length of the R substituent leads to a twist of the molecule around the central C–C bond. Furthermore, monoprotonation induces an asymmetry within the organic moieties as well as between the organic moieties and the tetrathionate ion. As in the case of **Mbqn^0-H$^+$**,[5] but less pronounced, the protonated side of each **Pbqn^0-H$^+$** adopts a rather stiffened quinoid type structure[5] with localised alternating long–short–long $N_1'–C_2'$, $C_2'–C_3'$ and $C_3'–C_3$ bond distances, respectively. In contrast, the non-protonated side of the molecule is rather aromatic with an opposite short–long–short trend in the corresponding bond distances (Figure 2). Furthermore, the presence of hydrogen bonds $N_2'–H\cdots O_1$ and $N_{2*}'–H\cdots O_2$ between the H–bond donor atoms (N_2', N_{2*}') of the organic species and the H–bond acceptor atom (O_1, O_2) of the tetrathionate ion is obvious. Indeed, in the hypothesis of non-protonation of the organic moieties the $N_2\cdots O_1$ and $N_2'\cdots O_1$ interatomic distances (same features for $N_{2*}\cdots O_2$ and $N_{2*}'\cdots O_2$) should, in principle, be equal (symmetrical situation with no preferred interactions between the organic species and the tetrathionate). In fact, the $N_2'\cdots O_1$ and $N_{2*}'\cdots O_2$ distances are much shorter than the $N_2\cdots O_1$ and $N_{2*}\cdots O_2$ respectively by about 0.19–0.34 Å which is in line with our suggestion that the intermediate purple species with R = propyl is the monoprotonated form **Pbqn^0-H$^+$**.

In order to oxidise the purple solid containing **Rbqn^0-H$^+$**, this was partially dissolved in 1:1 DMF/acetic acid mixture and stirred 30 min in air. Any remaining solid was filtered and washed with acetic acid. The resulting dark yellow filtrate was acidified with HBF_4 thus precipitating the *N,N*′-diquaternised biquinoxens, [**Rbqn^{2+}**]$(BF_4)_2$, as pale yellow/off-white crystalline salts in yields up to 32%.

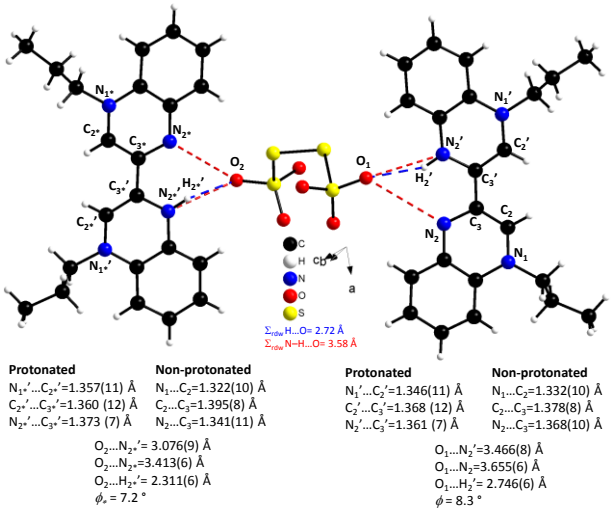

Fig. 2 Ball & Stick view of the asymmetric unit of [**Pbqn^{0}-H^{+}**]$_2$($S_4O_6^{2-}$). Salient C–C, C–N, O–N, O…H distances and dihedral angle ϕ=C_2–C_3–C_3'–C_2' are indicated.

Each compound was characterised by ^{1}H and ^{13}C NMR, electronic and IR spectroscopy as well as FAB mass spectrometry. **Mbqn^{2+}**, **Ebqn^{2+}** and **Bzbqn^{2+}** have been also identified by single crystal and powder X-ray diffraction and correspond to [**Mbqn^{2+}**]$(BF_4)_2$·MeCN, [**Ebqn^{2+}**]$(BF_4)_2$ and [**Bzbqn^{2+}**]$(BF_4)_2$·2MeCN, respectively. Crystals of **Pbqn^{2+}** were heavily twinned precluding any structure determination.

Possible Mechanism. Under anaerobic conditions the reaction of the *N*-alkylquinoxalinium cation with dithionite gives a dark blue solution accompanied by the formation of the *N,N'*-diquaternised biquinoxens, first isolated in their intermediate cationic direduced monoprotonated forms. These features are in line with an oxidative radical homocoupling between two chemically reduced *N*-alkylquinoxalinium rings, as suggested by Chupakhin *et al.* when studying quinoxaline ring dimerisation (Fig. 3).[7,12] In their proposed mechanism, by monoprotonating the quinoxaline the carbon alpha to the ammonium function becomes sufficiently electron deficient for a subsequent nucleophilic substitution of the hydrogen in the aromatic system. When the reaction is carried out under an inert atmosphere, the homolytic σ-decomposition of the intermediate species leads to the formation of a 1,4-

dihydroquinoxalinyl radical cation, which subsequently couples to give the biquinoxalinium species after oxidation.[7, 12]

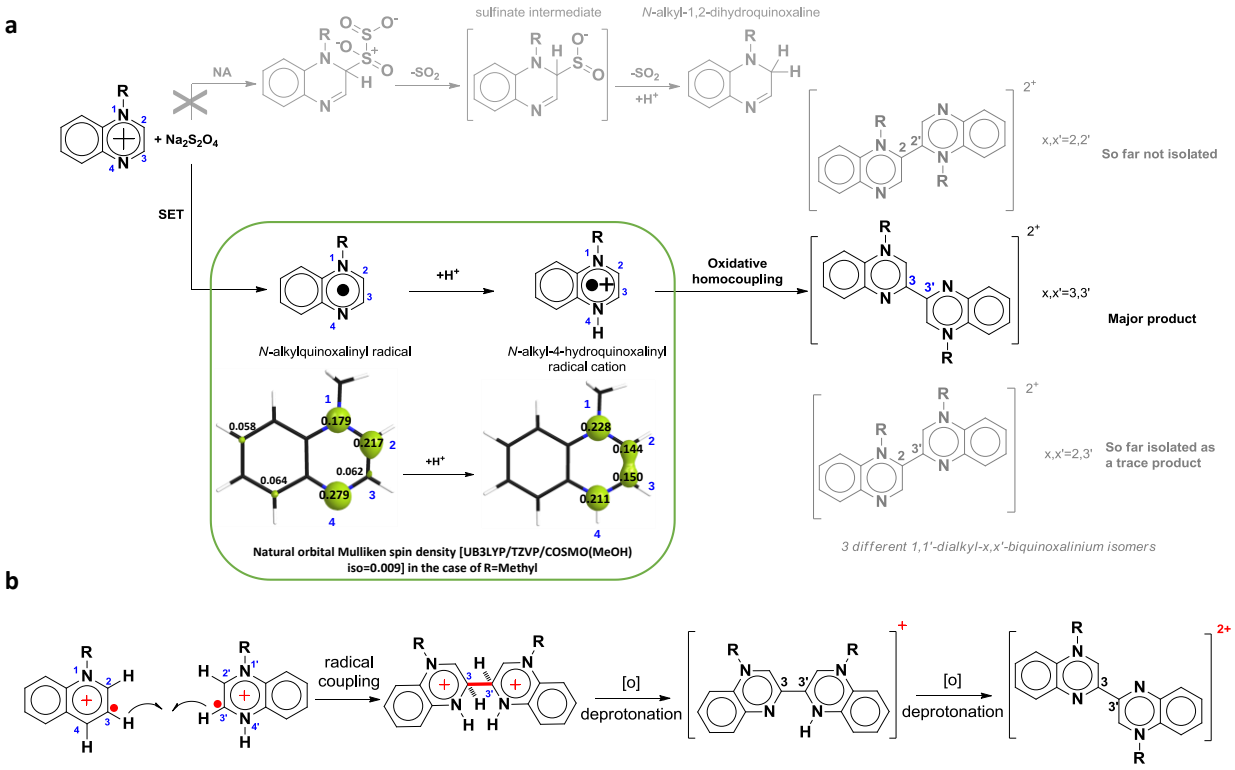

Fig. 3 Proposed mechanism of oxidative radical homocoupling for the synthesis of *N,N′*-diquaternised biquinoxen dications **Rbqn^{2+}** (R = Me, Et, Pr, Bz). a) A single electron transfer (SET) occurs between dithionite ($S_2O_4^{2-}$) and a *N*-alkylquinoxalinium cation leading to a *N*-alkylquinoxalinyl radical. Subsequent protonation gives the *N*-alkyl-4-hydroquinoxalinyl radical cation, which after oxidative homocoupling gives the *N,N′*-dialkyl-3,3′-biquinoxaliniun **Rbqn^{2+}** isomers as the major product. b) Scheme of the radical homocoupling followed by partial oxidation of the x,x′ = 3,3′ isomer, leading to the stable intermediates **Rbqn^{0}-H^{+}** which by complete oxidation give the *N,N′*-diquaternised biquinoxen dications, **Rbqn^{2+}**.

In our system, we propose a similar mechanism involving the *N*-alkyl-4-hydroquinoxalinyl radical cation as a key intermediate (Fig. 3). The *N*-alkylquinoxalinium cation is first reduced by sodium dithionite ($Na_2S_2O_4$). This is known to proceed via two different mechanisms.[13] Here, one possibility

involves the nucleophilic addition (NA) of the $S_2O_4^{2-}$ anion on the carbon alpha to the ammonium function (C_2) to form the sulfinate intermediate, which would then be reduced to the *N*-methyl-1,2-dihydroquinoxaline species by loss of SO_2 (Fig. 3a). So far such a reduced species could not be identified in our experiments. The second reduction mechanism involves only a single electron transfer (SET) from the dithionite to the *N*-alkylquinoxalinium cation leading to the *N*-alkylquinoxalinyl radical (Fig. 3a). In fact, we favour this SET from dithionite since it is a common technique used to generate radical species of *N*-substituted electron deficient cationic heterocycles.[14-16]

EPR Spectroscopy. The SET mechanism leads to the formation of an *N*-alkyl-4-hydroquinoxalinyl radical as we confirmed by EPR spectroscopy. Reduction of *N*-methylquinoxalinium with $Na_2S_2O_4$ in MeOH, DMF or DMSO results in the immediate formation of a dark plum reaction mixture characterised by a multiline EPR spectrum in all cases (Fig. 4). The signal is consistent with an $S = {}^1/_2$ *N*-alkyl-4-hydroquinoxalinyl whose rich hyperfine pattern stems from the inequivalence of its eight protons (^{1}H, $I = {}^1/_2$, ~100% abundant) and two nitrogens (^{14}N, $I = 1$, ~100% abundant). However, EPR is not able to differentiate between hydroquinoxalinyl and quinoxalinyl radical forms unlike in the more symmetric pyrazinyl analogue that gave a less dense splitting profile which confirmed the presence of the protonated species. Nevertheless, this signal is in stark contrast to the reduced homocoupled product, **MBqn$^{\bullet+}$-H$^+$**,[5] which gives its signature 9-line spectrum in DMF and DMSO solution (Fig. 4). The most realistic scenario is that the radical is protonated in solution since as is commonly observed when reducing similar *N*-monoquaternised cationic 1,4-diazine heterocycles with dithionite such as *N*-methylpyrazinium.[14,17-19]

To explore this further we compared the spin density distribution of the *N*-alkyl-4-hydroquinoxalinyl radical and the corresponding radical cation in solution (B3LYP/TZVP/COSMO level of theory). We especially focused on R = Me, *i.e.* the *N*-methyl-4-hydroquinoxalinyl radical and corresponding radical cation, using the structural parameters of the simple *N*-methylquinoxalinium cation.[20] The behaviour of the other *N*-quaternised quinoxalinium salts are most probably identical. As shown in the inset of Fig. 3a

the spin density of the neutral *N*-methylquinoxalinyl radical is mostly located on the atoms N_1, N_4 and C_2. As reported for other radical coupling reactions,[21] the nearly zero spin density on C_3 cannot explain a direct or at least efficient radical coupling between two C_3 atoms, which is however observed experimentally through the formation of the central C_3–C_3' sigma bond in both the organic species **Rbqn^0-H$^+$** and **Rbqn^{2+}**. In contrast, the protonation of the *N*-methylquinoxalinyl radical giving the *N*-methyl-4-hydroquinoxalinyl radical cation (Fig. 3a, inset) results in a better distribution of the spin density on C_3 which definitely favours such a radical coupling between two C_3 atoms.

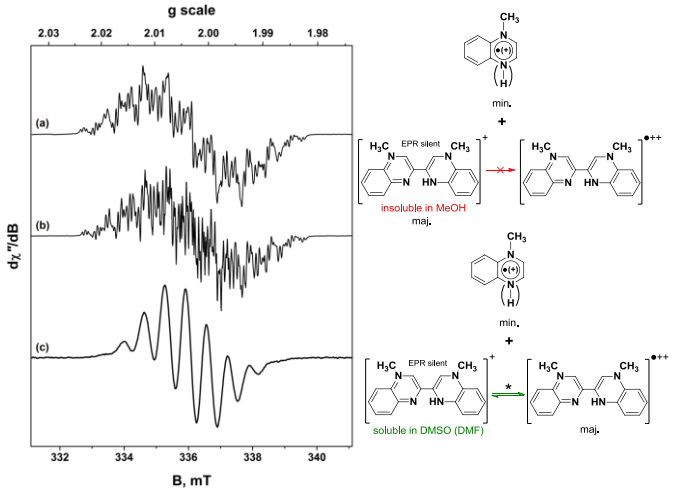

Fig. 4 (Left) Comparison of the X-band EPR spectra obtained from the reduction of *N*-methylquinoxalinium iodide: (a) in methanol; (b) in DMSO after 30 min; (c) in DMSO after 24 h. Experimental conditions: frequency, 9.423 GHz; modulation, 0.05 mT; power, 20 mW. (Right) Scheme representing the relationship between the EPR signals and the different species in presence after 24 h of reaction in MeOH (top) and DMSO (bottom). *Features already observed in ref 5.

Regioselectivity Aspects. The symmetric nature of the 1,4-dihydroquinoxalinyl radical cation studied by Chupakhin et al. leads to a single biquinoxalinium product after oxidative radical coupling.[7,12] In contrast, due to the asymmetric nature of the *N*-alkyl-4-hydroquinoxalinyl radical cation and the fact that the spin density on both C_2 and C_3 carbons is essentially the same, the oxidative radical coupling should be, in principle, non regioselective. Although this should theoretically give three different *N*,*N*′-dialkyl-

x,x′-biquinoxalinium isomers (abbreviated as x,x′), depending on which carbon atoms form the central bond (isomers x,x′ = 2,2′, 2,3′ or 3,3′ – Fig. 3a), this will depend on the chemical stability of the species towards oxidation and/or to the possibility to isolate these through fractional crystallisation. So far, the x,x′ = 2,2′ isomer has not been isolated, while a single crystal of an x,x′ = 2,3′ isomer – *N*,*N*′-diethyl-2,3′-biquinoxalinium – has been obtained only in its fully oxidised dicationic form under reducing conditions. In contrast, the x,x′ = 3,3′ isomers are systematically isolable in their partly oxidised form **Rbqn^{0}-H^{+}**, thus giving pure phases of **Rbqn^{2+}** after a simple aerial oxidation step. In short, although the disadvantage is that the coupling reaction is not regioselective, which might explain a maximum yield limited to 1/3 (1 isomer over 3; maximum yield of 32% observed (ESI)), the huge advantage is that the 3,3′-isomers "Biquinoxens" are easily isolable without any further purification step.

As a possible explanation for why it is possible only to crystallise the x = 3,3′ species from the intermediate step, from our experience on **Mbqn^{0}-H^{+}**[5] as well as from previous investigations on the effect of steric hindrance in radical coupling reactions[22,23] and on the ease of reduction, *i.e.* radical stability, of geometrically restrained viologens,[24] all indicate that the x,x′ = 3,3′ isomer is the only form which can be stabilised in solution in its reduced state compared with x,x′ = 2,2′ and 2,3′. This is in part due to the stabilising factors of perfect planarity of the molecule and a full π-electron delocalisation. These are in line with the most stable configuration of the direduced species where the π-electron density is paired on the central C_3-C_3′ bond.[5] In the case of x,x′ = 2,2′ and 2,3′ the fact that a more sterically hindered C_2 atom is involved can strongly disfavour the coupling reaction[22,23] and/or decrease the radical stability of the direduced species by inducing a significant twist of the molecule around the central C_2–C_2′ (C_3′) bond.[24]

Furthermore, the insolubility of the x,x′ = 3,3′ isomers **Rbqn^{0}-H^{+}** in MeOH greatly enhances the yield of the reaction compared to other solvents. As mentioned above, EPR confirmed the observation of the *N*-alkyl-4-hydroquinoxalinyl radical species (ESI) in MeOH, DMF and DMSO with a qualitative rate of colour change of the solution to dark blue (radical formation) increasing in the order MeOH < DMF < DMSO, which is in line with a better solubility of sodium dithionite in DMSO rather than in MeOH

(Fig. 4). However, as already known for **Mbqn^{0}-H**$^{+}$[5] the much better solubility of **Rbqn^{0}-H**$^{+}$ in DMF or DMSO precludes precipitation of the **Rbqn^{0}-H**$^{+}$ form which remains in solution in equilibrium with the corresponding radical **Rbqn$^{\bullet+}$-H**$^{+}$. Thus, this explains the non-measurable yields reported using DMF or DMSO solvents, the best yields being exclusively obtained in MeOH.

Counterion Influence on Yield. The influence of the anion on the reaction yield has also been investigated (ESI). It is clear that the counter ion plays a significant role with an increase in the yield of the [**Rbqn^{2+}**]$(BF_4)_2$ species (R = methyl, ethyl and benzyl) from 9% to 32% in the order of starting anions $I^- < Br^- < PF_6^-$. This is in line with the fact that I^- ions are more oxidisable and have a higher degree of ion pairing compared to Br^- and also PF_6^- ions. This favours quenching reactions involving iodide-mediated charge/electron transfer or radical scavenging mechanisms.[25-28]

However, the low yields observed in the case of R = propyl, either starting from I^- or PF_6^-, suggest that the isolation of the [**Rbqn^{2+}**]$(BF_4)_2$ species also depends on the intrinsic solubility of the biquinoxen dications which in turn is governed by the type of R substituent. Further experiments will be performed in future investigating these aspects in order to optimise the yields of the reactions.

Conclusions

In conclusion we have reported the oxidative radical homocoupling of chemically reduced *N*-alkylquinoxalinium salts as an alternative method for the synthesis of *N*,*N*′-diquaternised-3,3′-biquinoxalinium "biquinoxens" dications. Although referring back to figure 1 it is clear that left hand route can provide much better yields. This critically relies on the availability of the corresponding oxonium derivatives. The right hand route, despite non regioselectivity, still provides yields of up to 32%. Since this method is very simple it allows for gram scale synthesis at room temperature whilst using inexpensive reagents, no metal catalysts and no purification steps. Furthermore, the chemistry of the quinoxaline quaternary salts used here is more accessible than that of biquinoxaline, the previously reported starting reagent. This provides exciting prospects for simple access to new members of the

Biquinoxen family bearing various electron withdrawing/donating and possibly chiral groups as well as coordination functions.

Acknowledgment. The authors thank the financial support provided by the Alexander von Humboldt Foundation (fellowship to N.L) and Helmholtz POF "STN". We also thank Ingrid Freuze for the mass spectrometry measurements and Sven Stahl for the elemental analysis measurements.

References

†Electronic supplementary information (ESI) available: complete synthesis, tables of crystal and X-Ray crystallographic files in CIF format, XRPD patterns, UV-Vis and IR spectra of $[Rbqn^{2+}](BF_4)_2$ (R = Me, Et, P, Bz), additional EPR spectra, elemental analysis and DFT calculation of the intermediate species. CCDC 1511787–1511789. For ESI and crystallographic data in CIF or other electronic format see DOI: 10.1039/c000000x.

1. P. M. S. Monk, *The Viologens: Physicochemical Properties, Synthesis, and Application of the Salts of 4,4'-Bipyridine*, Wiley, 1998.
2. W. Kaim and W. Matheis, *Chem. Ber.*, 1990, **123**, 1323−1325.
3. W. Matheis and W. Kaim, *J. Chem. Soc., Faraday Trans.*, 1990, **86**, 3337−3339.
4. W. Matheis, J. Poppe, W. Kaim and S. Zalis, *J. Chem. Soc., Perkin Trans. 2*, 1994, 1923−1928.
5. N. Leblanc, S. Sproules, K. Fink, L. Sanguinet, O. Aleveque, E. Levillain, P. Rosa and A. K. Powell, *Chem. Sci.*, 2016, **7**, 3820-3828.
6. N. Leblanc, L. De Cola, D. Genovese and A. K. Powell, *Phys. Chem. Chem. Phys.*, 2016, DOI: 10.1039/C6CP07538J.
7. O. N. Chupakhin, E. O. Sidorov, S. M. Shein and I. I. Bil'kis, *Zh. Org. Khim.*, 1976, **12**, 2464−2468.
8. I. M. Piglosiewicz, R. Beckhaus, G. Wittstock, W. Saak and D. Haase, *Inorg. Chem*, 2007, **46**, 7610-7620.
9. C. M. Fitchett and P. J. Steel, *Polyhedron*, 2008, **27**, 1527-1537.
10. S.-R. Guo, P. S. Kumar and M. Yang, *Adv. Synth. Catal.*, 2016, DOI: 10.1002/adsc.201600467.
11. G. W. H. Chesseman and R. F. Cookson, in *The Chemistry of Heterocyclic Compounds, Condensed Pyrazines*, John Wiley & Sons, Inc., 2008, ch. 17, pp. 247-260.
12. O. N. Chupakhin and I. Y. Postovskii, *Russ. Chem. Rev.*, 1976, **45**, 454.
13. S. K. Chung, *J. Org. Chem*, 1981, **46**, 5457-5458.
14. D. R. Eaton, J. M. Watkins and R. J. Buist, *J. Am. Chem. Soc.*, 1985, **107**, 5604−5609.

15. T. M. Bockman and J. K. Kochi, *J. Org. Chem.*, 1990, **55**, 4127-4135.

16. N. Kitamura, Y. Nambu and T. Endo, *J. Polym. Sci. Pol. Chem.*, 1990, **28**, 3137-3143.

17. T. Yutaka, A. Kazuyuki, I. Toshiaki, K. Hitomi and I. Kazuhiko, *Chem. Lett.*, 1972, **1**, 847−848.

18. L. Roullier and E. Laviron, *Electrochim. Acta*, 1980, **25**, 795−804.

19. W. Kaim, *Res. Chem. Intermediat.*, 1987, **8**, 247−286.

20. N. Leblanc, S. Sproules, C. Pasquier, P. Auban-Senzier, H. Raffy and A. K. Powell, *Chem. Commun.*, 2015, **51**, 12740-12743.

21. A. K. Sangha, J. M. Parks, R. F. Standaert, A. Ziebell, M. Davis and J. C. Smith, *J. Phys. Chem. B*, 2012, **116**, 4760-4768.

22. F. M. Beringer and S. A. Galton, *J. Org. Chem*, 1963, **28**, 3417-3421.

23. T. C. Tempesti, A. B. Pierini and M. T. Baumgartner, *New J. Chem.*, 2009, 33, 1523-1528.

24. A. C. Benniston, A. Harriman, P. Li, J. P. Rostron, R. W. Harrington and W. Clegg, *Chem. Eur. J.*, 2007, 13, 7838-7851.

25. D. Bethell, R. G. Compton and R. G. Wellington, J. *Chem. Soc., Perkin Trans. 2*, 1992, 147-148.

26. C. Imrie, T. A. Modro, E. R. Rohwer and C. C. P. Wagener, *J. Org. Chem.*, 1993, 58, 5643-5649.

27. M. Mac, J. Wirz and J. Najbar, *Helv. Chim. Acta*, 1993, 76, 1319-1331.

28. S. Jayaraman and A. S. Verkman, *Biophys. Chem.*, 2000, 85, 49-57.

An alternative method to access diverse *N,N'*-diquaternised-3,3'-biquinoxalinium "Biquinoxen" dications

Nicolas Leblanc[*a], Stephen Sproules[b], Annie K. Powell[*a,c]

Supporting Information

A. Synthesis

A_1- Synthesis of *N,N'*-diquaternised biquinoxens

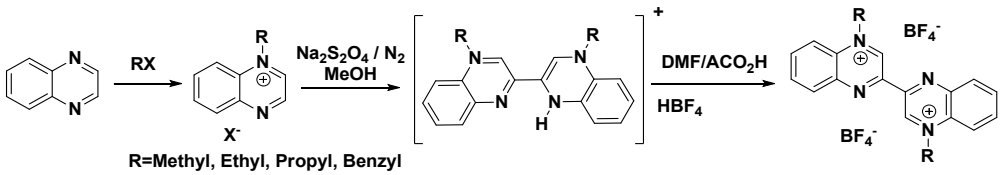

A_{11}- General Procedure

As detailed in the table hereafter, in a Schlenk round bottom flask were mixed the corresponding *N*-alkylquinoxalinium salt (RQ^+, X^-; R= Methyl (M), Et (E), Prop (P), Benzyl (Bz)), an excess of $Na_2S_2O_4$ and MeOH. The Schlenk was then purged with nitrogen, closed and inserted in an ultrasound bath for 15 min, thus giving a mixture which was left standing 7 days. The obtained purple crystalline powder was filtered, washed first with MeOH and then with distillate water and dried, leading to the direduced monoprotonated intermediate (**I**). The solid **I** was then dissolved in DMF under aerial conditions and left under agitation until the colour turned from dark blue/purple to "blood" red. Glacial acetic acid was added to the solution whilst stirring thus giving a mixture which, after 30 min stirring, was filtered and washed with glacial acetic acid until the filtrate turned dark yellow. To the dark yellow solution was added HBF_4 thus giving a precipitate of the title compound. The precipitation could be completed by adding THF. The solid was then filtered, washed with THF and dried under vacuum leading to the expected salts as a yellowish/off-white crystalline powder.

RQ^+,X^-	$Na_2S_2O_4$ (100%)	MeOH	Intermediate (I)	DMF	ACO_2H	HBF_4 50%	$RBqn(BF_4)_2$	Yield
MQ^+,I^- (2.18 g, 8 mmol)	2.18 g, 16.5 mmol	160 mL	0.769 g	14 mL	14 mL	35 mL	$MBqn(BF_4)_2$ 0.193 g	10 %
MQ^+,PF_6^-(1.15 g, 4 mmol)	1.45 g, 8.3 mmol	80 mL	0.333 g	6 mL	6 mL	15 mL	$MBqn(BF_4)_2$ 0.275 g	30 %
EQ^+,PF_6^-(1.23 g, 4 mmol)	1.45 g, 8.3 mmol	80 mL	0.683 g	12 mL	12 mL	30 mL	$EBqn(BF_4)_2$ 0.310 g	31 %
PQ^+,I^- (0.2 g, 0.7 mmol)	0.24 g, 1.4 mmol	17 mL	0.089 g	1.5 mL	1.5 mL	4 mL	$PBqn(BF_4)_2$ 0.016 g	9 %
PQ^+,PF_6^- (0.9 g, 2.8 mmol)	0.97 g, 5.6 mmol	70 mL	0.229 g	4 mL	4 mL	10 mL	$PBqn(BF_4)_2$ Fine powder very difficult to isolate	n.a
BzQ^+,Br^-(4.87 g, 16.2 mmol)	5.9 g, 33.9 mmol	320 mL	2.584 g	45 mL	45 mL	115 mL	$BzBqn(BF_4)_2$ 1.232 g	24 %
BzQ^+,PF_6^-(2.5 g, 6.8 mmol)	2.5 g, 14.3 mmol	140 mL	1.031 g	18 mL	18 mL	46 mL	$BzBqn(BF_4)_2$ 0.689 g	32 %

***N*-methylquinoxalinium iodide (MQ)[I].** Quinoxaline (5 mL, 4.32 10^{-2} mol) and methyliodide (4 mL, 6.42 10^{-2} mol) are mixed with 10 mL of DCM and the solution is left standing 3 weeks after sealing. The orange-red crystals formed are filtered, washed with Et_2O and dried under vacuum to afford 9.263 g (79%) of the tittle compound.

^1H NMR (500 MHz, DMSO-d^6): δ= 9.73 (d, J= 2.8 Hz, 1H), 9.67 (d, J= 2.8 Hz, 1H), 8.64 (d, J=8.5 Hz, 1H), 8.54 (dd, J=8.4, 1.3 Hz, 1H), 8.37 (ddd, J =8.7, 7.1, 1.5 Hz, 1H), 8.31 (ddd, J = 8.3, 7.1, 1.2 Hz, 1H), 4.73 (s, 3H).

***N*-ethylquinoxalinium iodide (EQ)[I].** In a round-bottomed flask is mixed quinoxaline (2 mL, 1.73 10^{-2} mol) with ethyliodide (2mL, 2.5 10^{-2} mol). After sealing, the solution is heated 48h at 60°C under stirring. After cooling down, Et_2O is added and the orange precipitate is then filtered, washed with Et_2O and dried, affording 2.525 g (51%) of the tittle compound.

^{1}H NMR (500 MHz, DMSO-d^6): δ= 9.72 (d, J= 2.9 Hz, 1H), 9.69 (d, J= 2.9 Hz, 1H), 8.74 (d, J=9 Hz, 1H), 8.55 (dd, J=8.4, 1.4 Hz, 1H), 8.35 (ddd, J =8.7, 7.0, 1.5 Hz, 1H), 8.29 (ddd, J = 8.2, 7.0, 1.2 Hz, 1H), 5.17 (q, J=7.2 Hz, 2H), 1.67 (t, J=7.3 Hz, 3H).

***N*-propylquinoxalinium iodide (PQ)[I].** In a round-bottomed flask is mixed quinoxaline (2 mL, 1.73 10^{-2} mol) with 1-iodopropane (6mL, 6.15 10^{-2} mol). After sealing, the system is purged with nitrogen and the solution is heated 48h at 70°C under stirring. After cooling down, Et_2O is added and the orange precipitate is then filtered, washed with Et_2O and dried, affording 1.56 g (30%) of the tittle compound.
^{1}H NMR (500 MHz, DMSO-d^6): δ= 9.73 (d, J= 2.6 Hz, 1H), 9.66 (d, J= 2.6 Hz, 1H), 8.77 (d, J=8.7 Hz, 1H), 8.55 (d J=7.8, 1H), 8.35 (ddd, J =7.3 Hz, 1H), 8.30 (ddd, J = 7.4, 1H), 5.10 (t, J=7.5 Hz, 2H), 2.07 (m, 7.4 Hz, 2H), 1.05 (t, J=7.3 Hz, 3H).

***N*-benzylquinoxalinium hexafluorophosphate (BzQ)[PF_6]**: A solution of quinoxaline (2.35 ml, 20 mmol) and benzylbromide (5 ml, 20mmol) is left standing 3 days, after what the dark yellow crystals are filtered, washed with Et_2O and dried affording *N*-benzylquinoxalinium bromide (BzQ)[Br] in a pure phase (3.34 g, 55%). (BzQ)[Br] (1 g, 3.3 mmol) is then dissolved in 30 ml of warm distillate water and subsequently poured into a stirring saturated aqueous solution of KPF_6 (1.22 g in 100 ml). The white crystalline precipitate is then filtered, washed with water and dried, leading to (BzQ)[PF_6] in a pure phase (0.98 g, 80 %). ^{1}H NMR (500 MHz, DMSO-d^6): δ = 9.79 (d, *J* = 2.8 Hz, 1H), 9.69 (d, *J* = 2.8 Hz, 1H), 8.63 (d, *J* = 8.3 Hz, 1H), 8.58 (dd, *J* = 8.1, 1.2 Hz, 1H), 8.39 – 8.19 (m, 2H), 7.55 (d, *J* = 6.5 Hz, 2H), 7.49 – 7.40 (m, 3H), 6.44 (s, 2H).

The ion exchange procedure aforementioned has been similarly applied to the other compounds.

A_{12}- $MBqn(BF_4)_2$

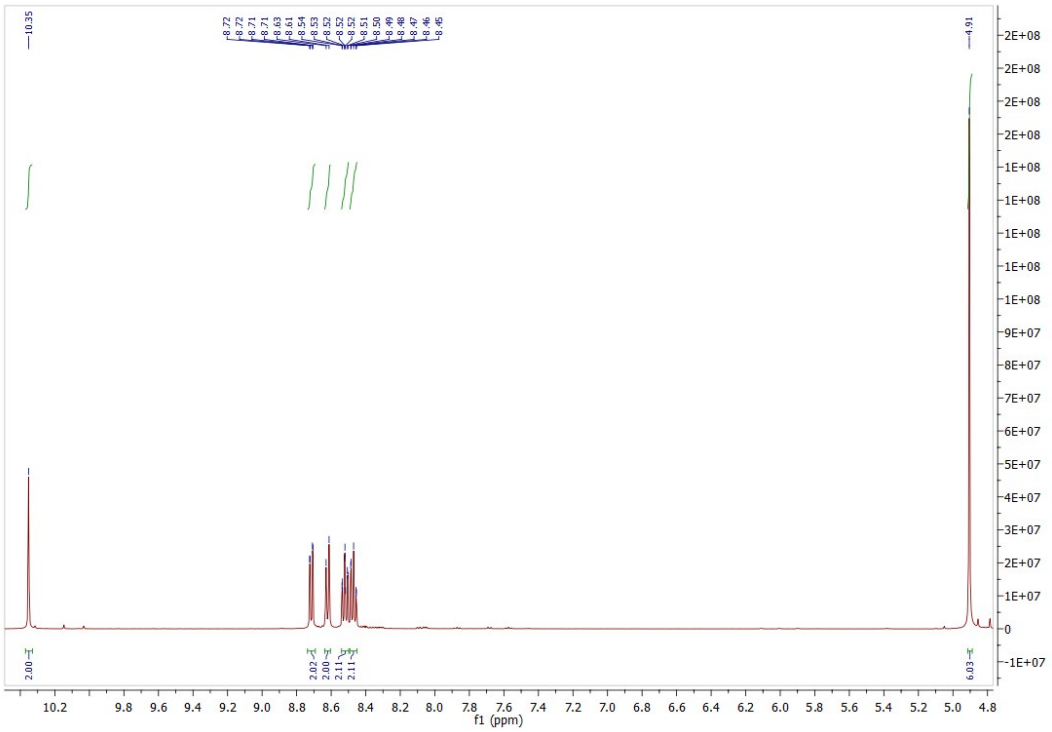

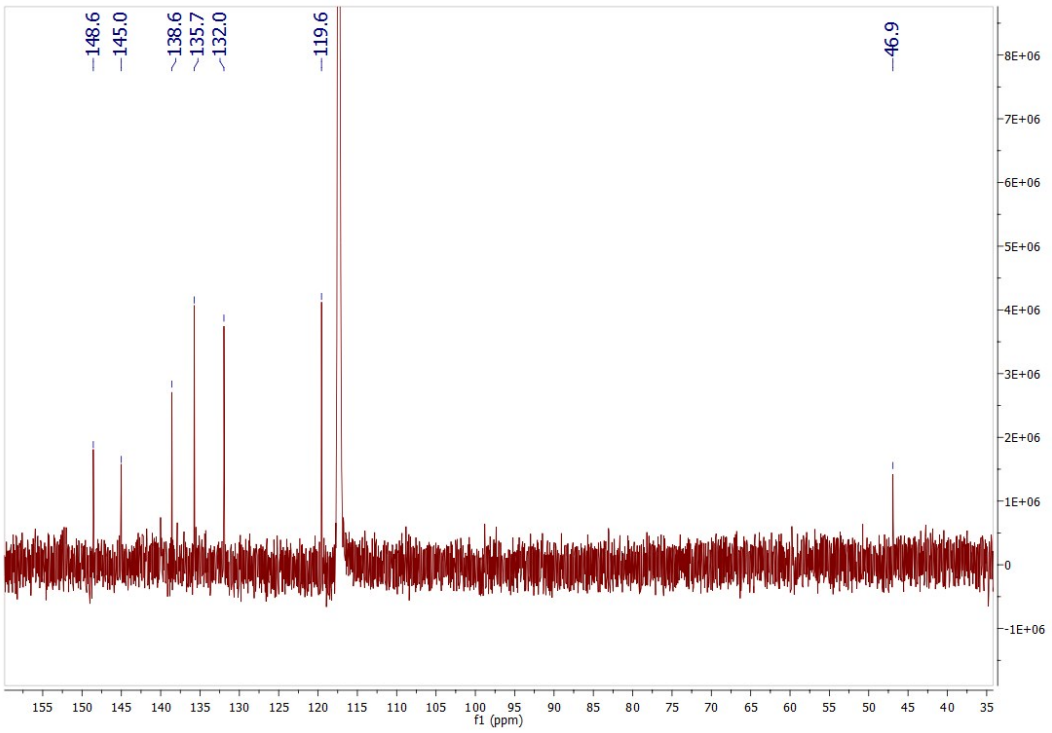

^{1}H NMR (500 MHz, CD_3CN): δ = 10.35 (s, 2H), 8.72 (dd, *J* = 8.3, 1.3 Hz, 2H), 8.62 (d, *J* = 8.6 Hz, 2H), 8.52 (ddd, *J* = 8.7, 7.1, 1.5 Hz, 2H), 8.49 – 8.45 (m, 1H), 4.91 (s, 6H). ^{13}C NMR (125 MHz, CD_3CN): δ = 148.6, 145.0, 138.6, 135.7, 132.0, 119.6, 46.9.

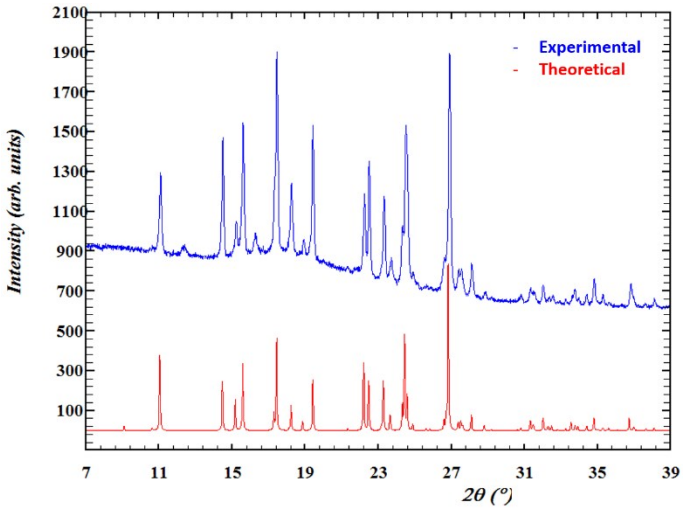

PXRD pattern of (Mbqn)$[BF_4]_2$. 2 MeCN

A_{13} - (Ebqn)$[BF_4]_2$

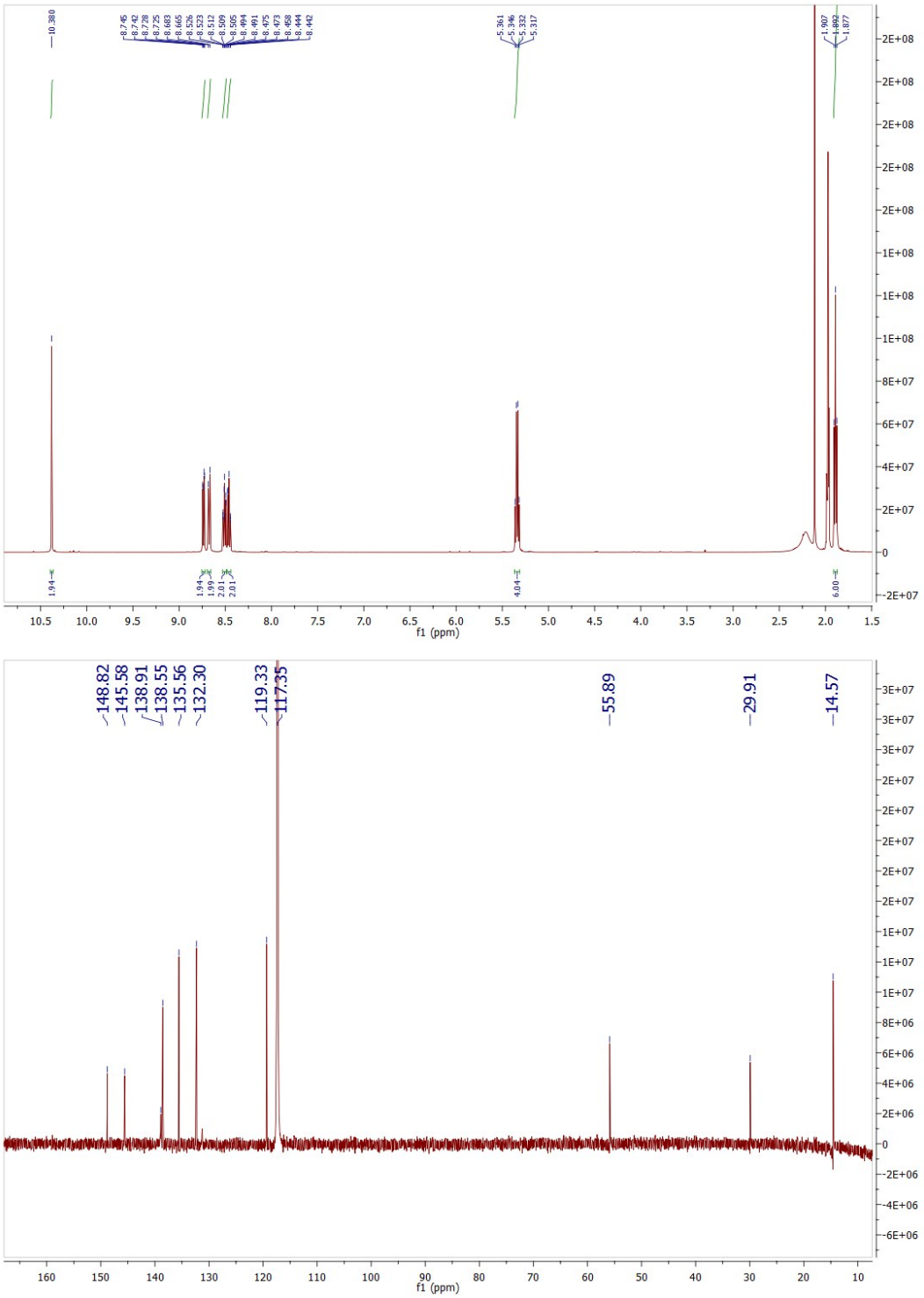

^{1}H NMR (500 MHz, CD_3CN): δ = 10.38 (s, 2H), 8.73 (dd, *J* = 8.3, 1.4 Hz, 2H), 8.67 (d, *J* = 8.6 Hz, 2H), 8.51 (ddd, *J* = 8.7, 7.1, 1.5 Hz, 2H), 8.46 (ddd, *J* = 8, 7.5, 1.5 Hz, 2H), 5.34 (q, *J* = 7.3 Hz, 4H), 1.89 (t, *J* = 7.3 Hz, 3H). ^{13}C NMR (125 MHz, CD_3CN): δ = 148.8, 145.6, 138.9, 138.5, 135.6, 132.3, 131.3, 119.3, 55.9, 14.6.

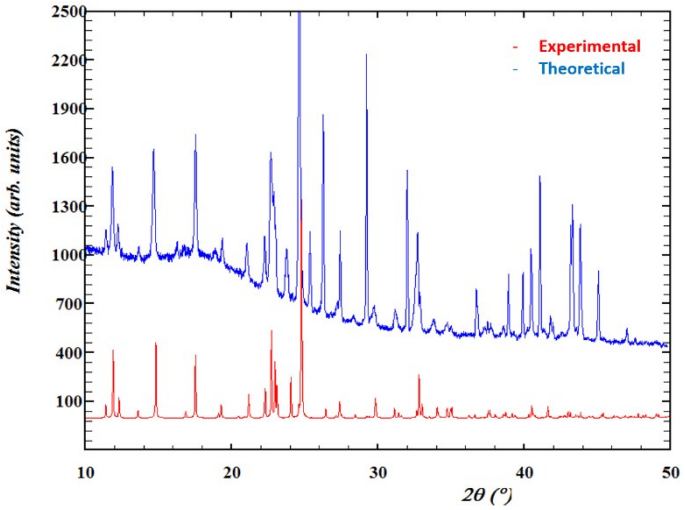

PXRD pattern of $(Ebqn)[BF_4]_2$

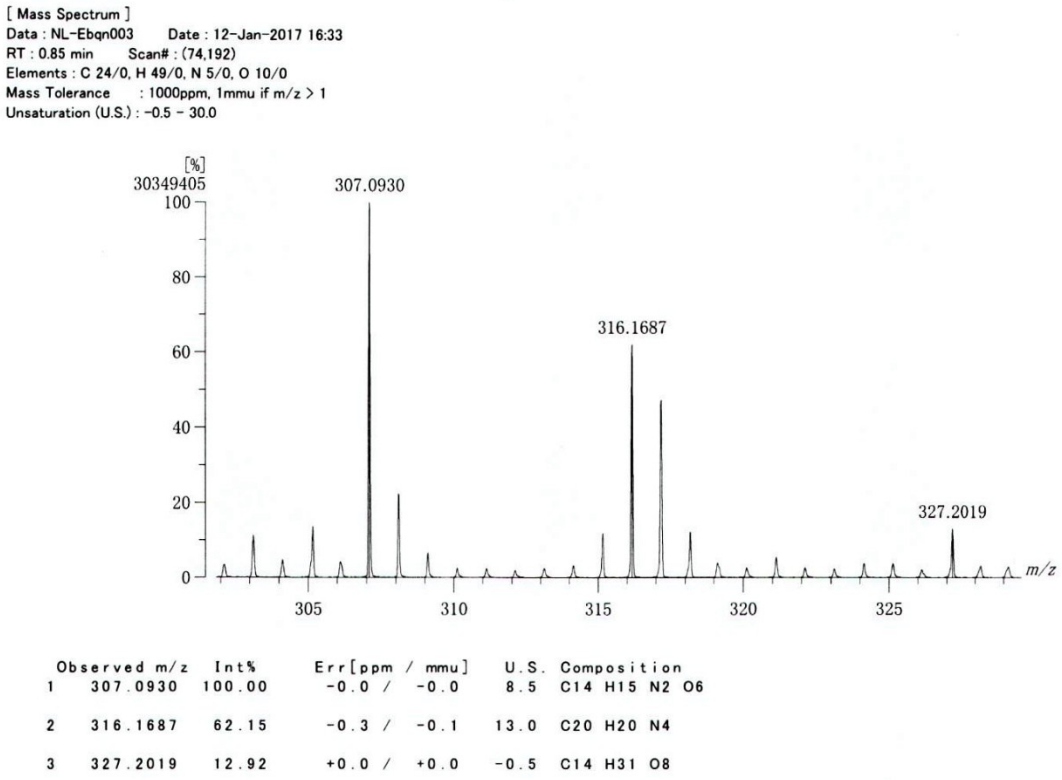

	Observed m/z	Int%	Err[ppm / mmu]	U.S.	Composition
1	307.0930	100.00	-0.0 / -0.0	8.5	C14 H15 N2 O6
2	316.1687	62.15	-0.3 / -0.1	13.0	C20 H20 N4
3	327.2019	12.92	+0.0 / +0.0	-0.5	C14 H31 O8

FAB mass spectrum of $(Ebqn)[BF_4]_2$. $M_{theo}(Ebqn^{2+})$=316.17 m/z

A_{13} - (Pbqn)$[BF_4]_2$

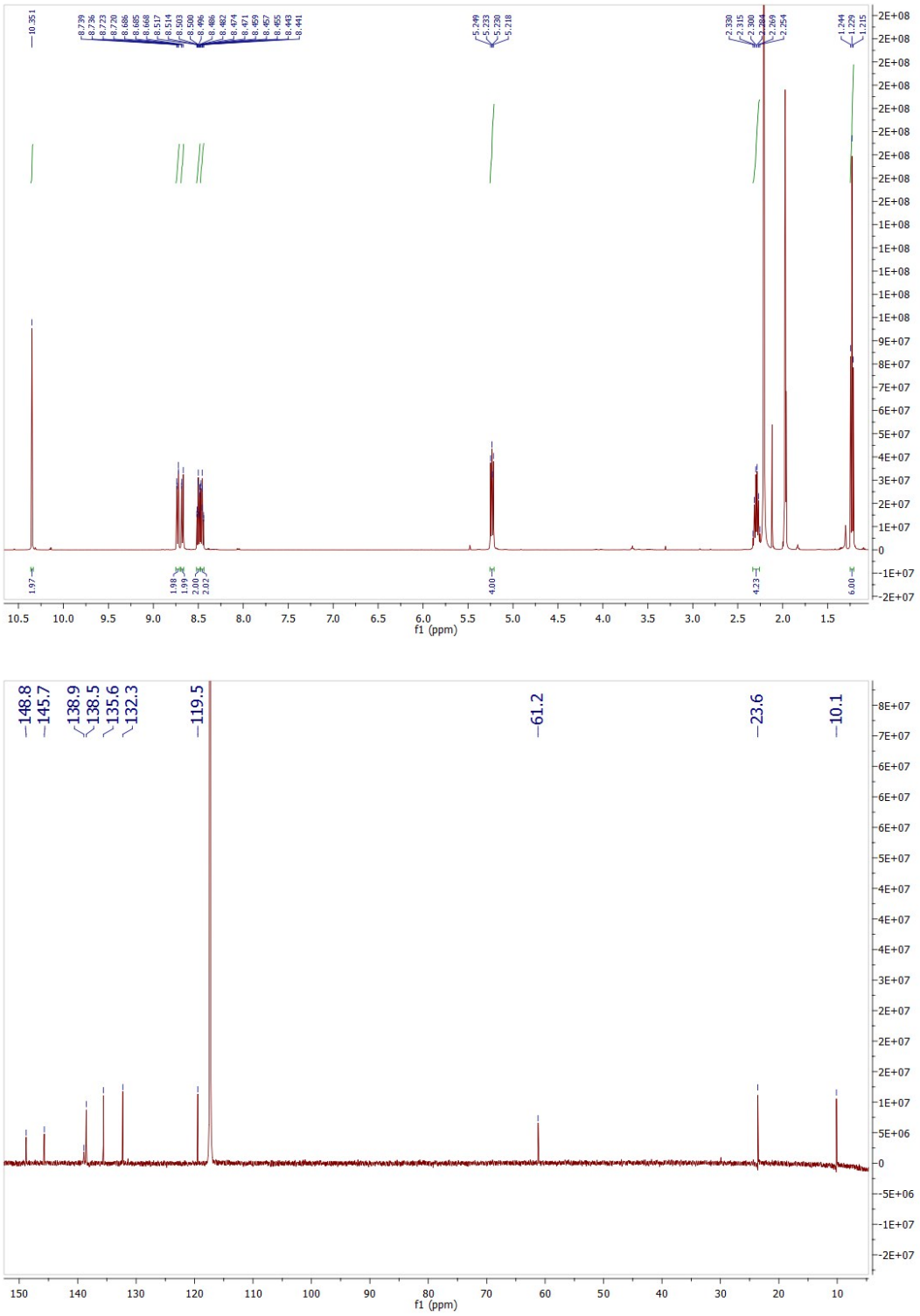

^{1}H NMR (500 MHz, CD_3CN): δ = 10.35 (s, 2H), 8.73 (dd, *J* = 8.3, 1.5 Hz, 2H), 8.68 (d, *J* = 8.5, 2H), 8.50 (ddd, *J* = 8.8, 7.0, 1.6 Hz, 2H), 8.46 (ddd, *J* = 8.1, 7.1, 1.2 Hz, 2H), 5.23 (t, *J* = 8.3 Hz, 4H), 2.29 (sex, *J* = 8, 7.5 Hz, 4H), 1.23 (t, *J* = 7.4 Hz, 6H) . ^{13}C NMR (125 MHz, CD_3CN): δ = 148.8, 145.7, 138.9, 138.5, 135.6, 132.3, 131.4, 119.5, 61.2, 23.6, 10.1.

[Mass Spectrum]
Data : NL-PBqn001 Date : 12-Jan-2017 16:46
RT : 1.57 min Scan# : (65,96)
Elements : C 24/0, H 49/0, N 5/0
Mass Tolerance : 1000ppm, 1mmu if m/z > 1
Unsaturation (U.S.) : -0.5 - 30.0

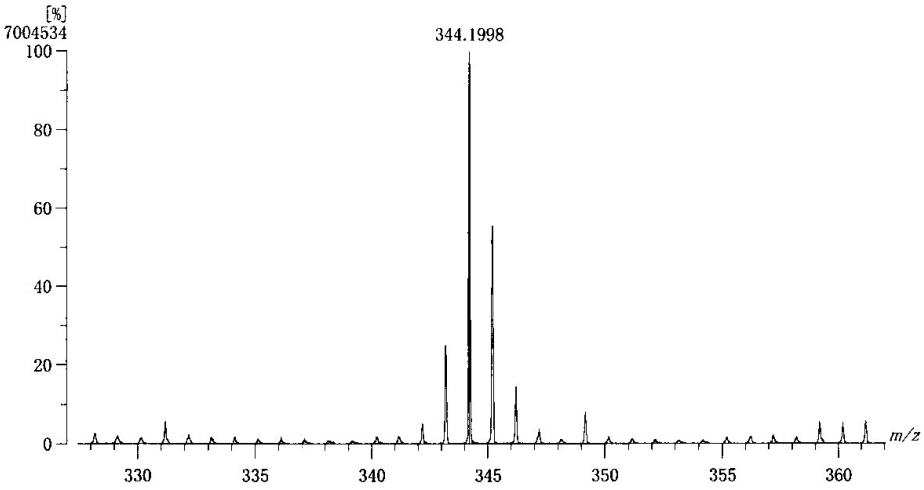

	Observed m/z	Int%	Err[ppm / mmu]	U.S.	Composition
1	344.1998	100.00	-0.9 / -0.3	13.0	C22 H24 N4

FAB mass spectrum of (Pbqn)$[BF_4]_2$. $M_{theo}(Pbqn^{2+})$=344.20 m/z

A_{14} - (Bzbqn)$[BF_4]_2$

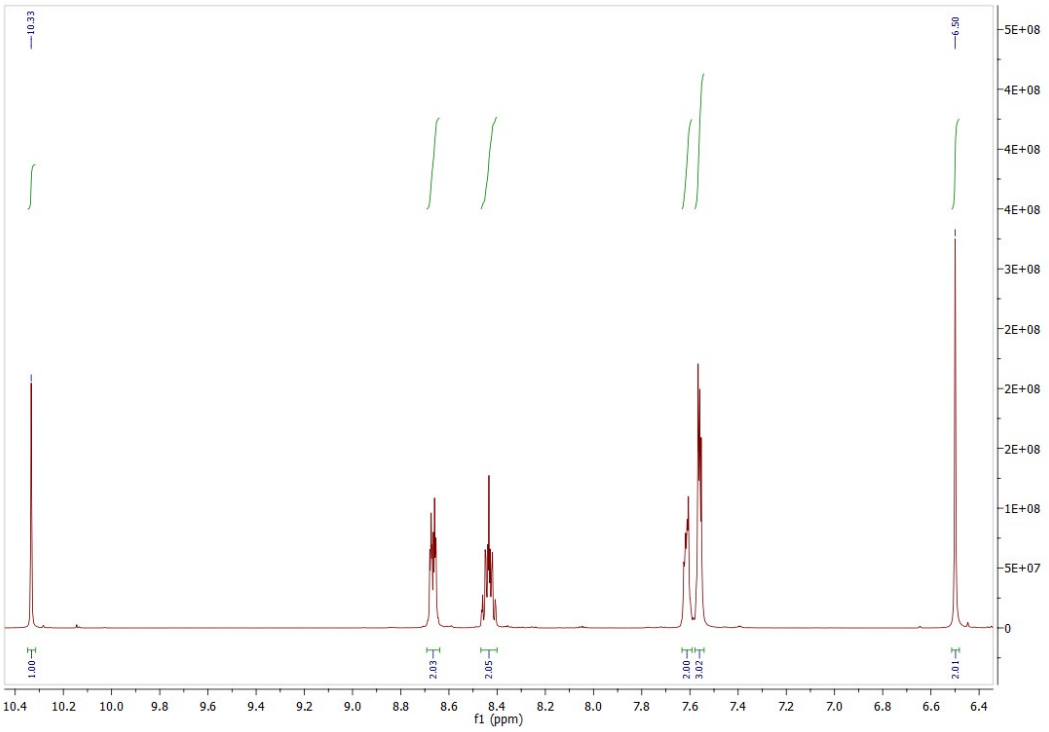

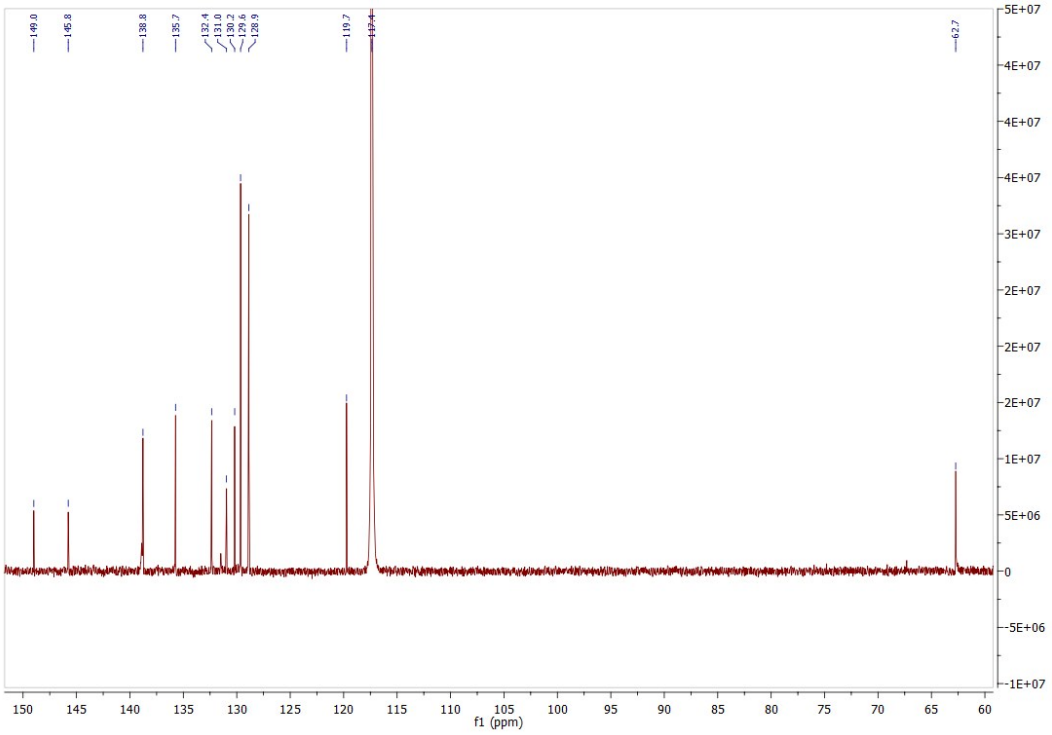

(Bzbqn)$[BF_4]_2$. 2MECN: ^{1}H NMR (500 MHz, CD_3CN): δ = 10.33 (s, 2H), 8.67 (m, 4H), 8.43 (m, 4H), 7.61 (dt, *J* = 6.1, 3.6 Hz, 4H), 7.56 (dd, *J* = 6.8, 3.5 Hz, 6H), 6.50 (s, 4H). ^{13}C NMR (125 MHz, CD_3CN): δ = 149.0, 145.8, 138.8, 138.5, 135.7, 132.3, 131.0, 130.2, 129.6, 128.9, 119.7, 62.7.

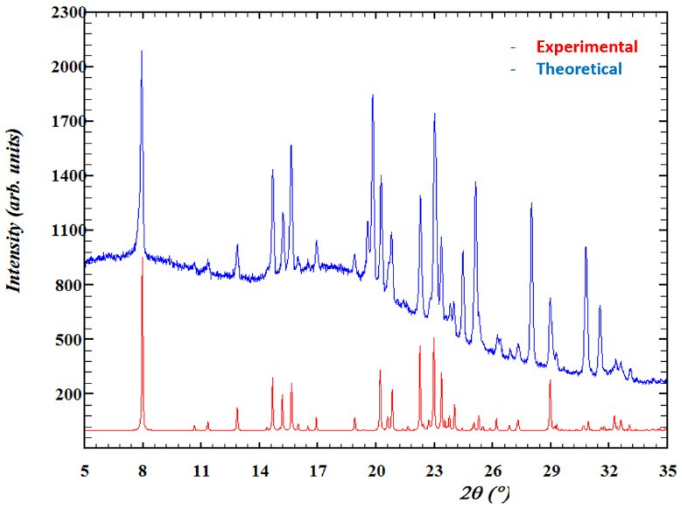

PXRD pattern of (Bzbqn)$[BF_4]_2$ .2 MeCN

[Mass Spectrum]
Data : NL-BzBqn002 Date : 12-Jan-2017 17:03
RT : 0.83 min Scan# : (35,47)
Elements : C 30/18, H 49/0, N 5/0, O 15/0
Mass Tolerance : 1000ppm, 1mmu if m/z > 1
Unsaturation (U.S.) : -0.5 - 30.0

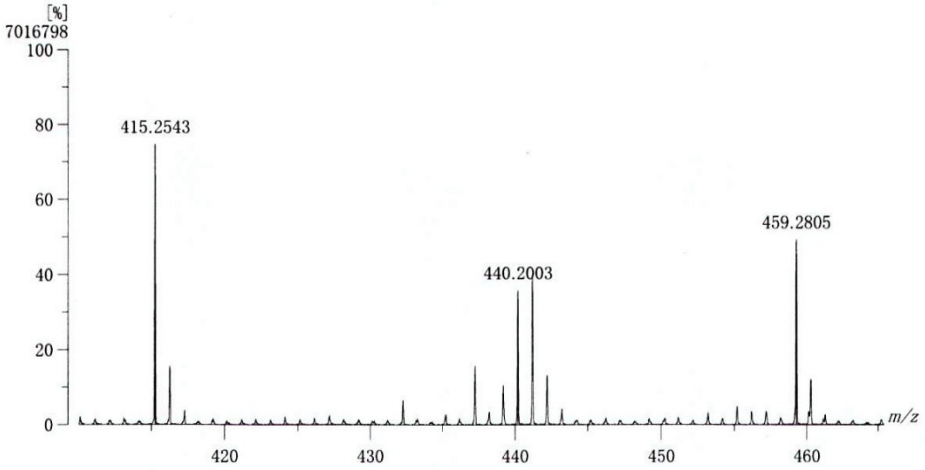

	Observed m/z	Int%	Err[ppm / mmu]	U.S.	Composition
1	415.2543	74.70	-0.1 / -0.0	-0.5	C18 H39 O10
2	440.2003	35.76	+0.5 / +0.2	21.0	C30 H24 N4
3	459.2805	49.29	-0.1 / -0.0	-0.5	C20 H43 O11

FAB mass spectrum of $(Bzbqn)[BF_4]_2$. $M_{theo}(Bzbqn^{2+})$=440.20 m/z

B. Single crystal X-ray diffraction analysis for $(Mbqn)[BF_4]_2$. MeCN, $(Ebqn)[BF_4]_2$ and $(Bzbqn)[BF_4]_2$. 2 MeCN

B_{11} - $(Mbqn)[BF_4]_2$. MeCN

Empirical formula	C20 H16 B2 F8 N5
Formula weight	500.00
Temperature	291(2) K
Wavelength	0.71073 A
Crystal system, space group	Monoclinic, C 2/c
Unit cell dimensions	a = 19.372(2) A alpha = 90 deg. b = 12.2295(10) A beta = 124.421(8) deg. c = 11.3742(14) A gamma = 90 deg.
Volume	2222.8(5) A^3
Z, Calculated density	4, 1.494 Mg/m^3
Absorption coefficient	0.137 mm^-1
F(000)	1012
Crystal size	0.385 x 0.367 x 0.344 mm
Theta range for data collection	2.097 to 27.415 deg.
Limiting indices	-24<=h<=18, -15<=k<=13, -14<=l<=14
Reflections collected / unique	5009 / 2438 [R(int) = 0.0217]
Completeness to theta = 25.242	96.7 %
Absorption correction	None
Refinement method	Full-matrix least-squares on F^2
Data / restraints / parameters	2438 / 0 / 194
Goodness-of-fit on F^2	1.124
Final R indices [I>2sigma(I)]	R1 = 0.0617, wR2 = 0.1976
R indices (all data)	R1 = 0.0760, wR2 = 0.2127
Extinction coefficient	n/a
Largest diff. peak and hole	0.308 and -0.233 e.A^-3

Table 2. Atomic coordinates (x 10^4) and equivalent isotropic displacement parameters (A^2 x 10^3) for mbqn.
U(eq) is defined as one third of the trace of the orthogonalized Uij tensor.

	x	y	z	U(eq)
C(1)	6380(2)	3605(2)	7139(3)	70(1)
C(2)	7016(1)	3100(1)	5901(2)	53(1)
C(3)	7263(1)	2318(1)	5293(2)	51(1)
C(4)	6676(1)	951(1)	5815(2)	54(1)
C(5)	6498(1)	-168(2)	5791(2)	63(1)
C(6)	6099(1)	-518(2)	6391(2)	67(1)
C(7)	5864(1)	235(2)	7038(2)	69(1)
C(8)	6015(1)	1322(2)	7077(2)	64(1)
C(9)	6424(1)	1697(1)	6456(2)	53(1)
C(10)	5000	2969(3)	2500	78(1)
C(11)	5000	4148(3)	2500	122(2)
N(1)	6611(1)	2784(1)	6457(2)	53(1)
N(2)	7092(1)	1275(1)	5241(2)	55(1)
N(3)	5000	2058(3)	2500	115(1)
B(1)	8671(2)	1537(2)	9571(2)	70(1)
F(1)	8373(2)	598(2)	9715(3)	140(1)
F(2A)	8642(5)	1578(5)	8393(6)	143(2)
F(2B)	8358(11)	1924(16)	8379(13)	218(11)
F(3A)	8095(2)	2321(2)	9432(5)	107(1)
F(3B)	9395(7)	960(11)	9700(17)	214(6)
F(4A)	9359(2)	1837(6)	10743(5)	150(2)
F(4B)	9030(20)	2223(13)	10570(20)	198(10)

Table 3. Bond lengths [A] and angles [deg] for mbqn.

C(1)-N(1)	1.484(2)
C(2)-N(1)	1.313(2)
C(2)-C(3)	1.414(2)
C(3)-N(2)	1.311(2)
C(3)-C(3)#1	1.473(3)
C(4)-N(2)	1.353(2)
C(4)-C(5)	1.407(3)
C(4)-C(9)	1.415(3)
C(5)-C(6)	1.357(3)
C(6)-C(7)	1.406(3)
C(7)-C(8)	1.357(3)
C(8)-C(9)	1.405(3)
C(9)-N(1)	1.377(2)
C(10)-N(3)	1.115(5)
C(10)-C(11)	1.442(5)
B(1)-F(2B)	1.225(10)
B(1)-F(4B)	1.262(10)
B(1)-F(4A)	1.296(4)
B(1)-F(2A)	1.309(4)
B(1)-F(1)	1.336(3)
B(1)-F(3A)	1.411(4)
B(1)-F(3B)	1.502(10)
F(2A)-F(2B)	0.69(3)
F(2A)-F(3B)	1.568(15)
F(2B)-F(3A)	1.62(3)
F(3A)-F(4B)	1.53(3)
F(3B)-F(4A)	1.630(13)
F(4A)-F(4B)	0.72(3)
N(1)-C(2)-C(3)	119.75(16)
N(2)-C(3)-C(2)	122.21(16)
N(2)-C(3)-C(3)#1	118.68(18)
C(2)-C(3)-C(3)#1	119.11(19)
N(2)-C(4)-C(5)	118.78(16)
N(2)-C(4)-C(9)	122.15(16)

C(5)-C(4)-C(9)	119.06(17)
C(6)-C(5)-C(4)	119.94(18)
C(5)-C(6)-C(7)	120.16(19)
C(8)-C(7)-C(6)	122.01(19)
C(7)-C(8)-C(9)	118.49(19)
N(1)-C(9)-C(8)	122.51(16)
N(1)-C(9)-C(4)	117.16(15)
C(8)-C(9)-C(4)	120.32(17)
N(3)-C(10)-C(11)	180.0
C(2)-N(1)-C(9)	120.78(14)
C(2)-N(1)-C(1)	119.41(15)
C(9)-N(1)-C(1)	119.78(15)
C(3)-N(2)-C(4)	117.94(15)
F(2B)-B(1)-F(4B)	114.7(13)
F(2B)-B(1)-F(4A)	127.3(6)
F(4B)-B(1)-F(4A)	32.9(13)
F(2B)-B(1)-F(2A)	31.2(13)
F(4B)-B(1)-F(2A)	125.5(5)
F(4A)-B(1)-F(2A)	117.7(5)
F(2B)-B(1)-F(1)	119.4(6)
F(4B)-B(1)-F(1)	121.2(5)
F(4A)-B(1)-F(1)	112.5(3)
F(2A)-B(1)-F(1)	112.7(3)
F(2B)-B(1)-F(3A)	75.4(15)
F(4B)-B(1)-F(3A)	69.4(15)
F(4A)-B(1)-F(3A)	102.2(4)
F(2A)-B(1)-F(3A)	106.6(4)
F(1)-B(1)-F(3A)	103.2(3)
F(2B)-B(1)-F(3B)	98.0(15)
F(4B)-B(1)-F(3B)	102.4(15)
F(4A)-B(1)-F(3B)	70.8(6)
F(2A)-B(1)-F(3B)	67.4(6)
F(1)-B(1)-F(3B)	91.7(6)
F(3A)-B(1)-F(3B)	165.1(6)
F(2B)-F(2A)-B(1)	67.6(12)
F(2B)-F(2A)-F(3B)	128.6(14)
B(1)-F(2A)-F(3B)	62.2(5)
F(2A)-F(2B)-B(1)	81.2(9)
F(2A)-F(2B)-F(3A)	138.6(12)
B(1)-F(2B)-F(3A)	57.5(11)
B(1)-F(3A)-F(4B)	50.7(5)
B(1)-F(3A)-F(2B)	47.1(5)
F(4B)-F(3A)-F(2B)	83.4(6)
B(1)-F(3B)-F(2A)	50.4(4)
B(1)-F(3B)-F(4A)	48.7(4)
F(2A)-F(3B)-F(4A)	88.4(6)
F(4B)-F(4A)-B(1)	71.0(13)
F(4B)-F(4A)-F(3B)	128.9(15)
B(1)-F(4A)-F(3B)	60.5(5)
F(4A)-F(4B)-B(1)	76.1(8)
F(4A)-F(4B)-F(3A)	135.9(13)
B(1)-F(4B)-F(3A)	59.9(11)

Symmetry transformations used to generate equivalent atoms:
#1 -x+3/2,-y+1/2,-z+1

Table 4. Anisotropic displacement parameters (A^2 x 10^3) for mbqn.
The anisotropic displacement factor exponent takes the form:
-2 pi^2 [h^2 a*^2 U11 + ... + 2 h k a* b* U12]

	U11	U22	U33	U23	U13	U12
C(1)	84(1)	56(1)	96(1)	-7(1)	67(1)	2(1)
C(2)	56(1)	48(1)	60(1)	2(1)	36(1)	1(1)
C(3)	56(1)	48(1)	52(1)	2(1)	32(1)	2(1)
C(4)	57(1)	50(1)	55(1)	2(1)	33(1)	0(1)
C(5)	74(1)	50(1)	70(1)	1(1)	44(1)	-2(1)
C(6)	73(1)	55(1)	77(1)	4(1)	45(1)	-7(1)
C(7)	70(1)	70(1)	79(1)	7(1)	49(1)	-6(1)
C(8)	66(1)	65(1)	73(1)	1(1)	46(1)	-1(1)
C(9)	53(1)	51(1)	56(1)	4(1)	32(1)	0(1)
C(10)	76(2)	68(2)	92(2)	0	48(2)	0
C(11)	161(5)	60(2)	146(4)	0	88(4)	0
N(1)	57(1)	49(1)	60(1)	1(1)	37(1)	4(1)
N(2)	64(1)	50(1)	60(1)	0(1)	39(1)	0(1)
N(3)	125(3)	69(2)	183(4)	0	107(3)	0
B(1)	81(2)	59(1)	65(1)	1(1)	38(1)	-3(1)
F(1)	211(3)	67(1)	185(2)	-6(1)	137(2)	-26(1)
F(2A)	213(6)	154(4)	116(3)	-17(3)	126(4)	-21(3)
F(2B)	141(9)	209(12)	97(7)	96(8)	-57(7)	-92(8)
F(3A)	105(2)	74(2)	127(3)	6(2)	56(2)	29(1)
F(3B)	147(7)	238(12)	270(13)	-31(11)	125(9)	24(8)
F(4A)	68(2)	212(5)	105(2)	-17(3)	9(2)	-14(2)
F(4B)	400(30)	130(8)	182(12)	-106(8)	240(17)	-150(12)

Table 5. Torsion angles [deg] for mbqn.

N(1)-C(2)-C(3)-N(2)	1.0(3)
N(1)-C(2)-C(3)-C(3)#1	-178.42(18)
N(2)-C(4)-C(5)-C(6)	178.40(17)
C(9)-C(4)-C(5)-C(6)	-0.7(3)
C(4)-C(5)-C(6)-C(7)	-0.1(3)
C(5)-C(6)-C(7)-C(8)	0.7(3)
C(6)-C(7)-C(8)-C(9)	-0.4(3)
C(7)-C(8)-C(9)-N(1)	-179.36(18)
C(7)-C(8)-C(9)-C(4)	-0.4(3)
N(2)-C(4)-C(9)-N(1)	0.9(3)
C(5)-C(4)-C(9)-N(1)	179.99(16)
N(2)-C(4)-C(9)-C(8)	-178.16(16)
C(5)-C(4)-C(9)-C(8)	0.9(3)
C(3)-C(2)-N(1)-C(9)	0.1(3)
C(3)-C(2)-N(1)-C(1)	177.87(17)
C(8)-C(9)-N(1)-C(2)	178.05(17)
C(4)-C(9)-N(1)-C(2)	-1.0(2)
C(8)-C(9)-N(1)-C(1)	0.3(3)
C(4)-C(9)-N(1)-C(1)	-178.74(17)
C(2)-C(3)-N(2)-C(4)	-1.1(3)
C(3)#1-C(3)-N(2)-C(4)	178.34(18)
C(5)-C(4)-N(2)-C(3)	-178.97(17)
C(9)-C(4)-N(2)-C(3)	0.1(3)
F(4B)-B(1)-F(2A)-F(2B)	-79(2)
F(4A)-B(1)-F(2A)-F(2B)	-116.9(13)
F(1)-B(1)-F(2A)-F(2B)	109.6(12)
F(3A)-B(1)-F(2A)-F(2B)	-3.0(13)
F(3B)-B(1)-F(2A)-F(2B)	-168.5(14)
F(2B)-B(1)-F(2A)-F(3B)	168.5(14)
F(4B)-B(1)-F(2A)-F(3B)	89(2)
F(4A)-B(1)-F(2A)-F(3B)	51.6(7)
F(1)-B(1)-F(2A)-F(3B)	-81.9(6)
F(3A)-B(1)-F(2A)-F(3B)	165.5(6)
F(3B)-F(2A)-F(2B)-B(1)	-13.0(16)
B(1)-F(2A)-F(2B)-F(3A)	3.8(16)
F(3B)-F(2A)-F(2B)-F(3A)	-9(3)

F(4B)-B(1)-F(2B)-F(2A)	118.4(19)
F(4A)-B(1)-F(2B)-F(2A)	82.7(19)
F(1)-B(1)-F(2B)-F(2A)	-85.8(13)
F(3A)-B(1)-F(2B)-F(2A)	177.1(13)
F(3B)-B(1)-F(2B)-F(2A)	10.7(13)
F(4B)-B(1)-F(2B)-F(3A)	-58.6(15)
F(4A)-B(1)-F(2B)-F(3A)	-94.4(13)
F(2A)-B(1)-F(2B)-F(3A)	-177.1(13)
F(1)-B(1)-F(2B)-F(3A)	97.2(9)
F(3B)-B(1)-F(2B)-F(3A)	-166.4(6)
F(2B)-B(1)-F(3A)-F(4B)	-124.0(7)
F(4A)-B(1)-F(3A)-F(4B)	1.7(6)
F(2A)-B(1)-F(3A)-F(4B)	-122.4(6)
F(1)-B(1)-F(3A)-F(4B)	118.6(5)
F(3B)-B(1)-F(3A)-F(4B)	-59(2)
F(4B)-B(1)-F(3A)-F(2B)	124.0(7)
F(4A)-B(1)-F(3A)-F(2B)	125.7(6)
F(2A)-B(1)-F(3A)-F(2B)	1.6(7)
F(1)-B(1)-F(3A)-F(2B)	-117.4(5)
F(3B)-B(1)-F(3A)-F(2B)	65(2)
F(2A)-F(2B)-F(3A)-B(1)	-4.4(19)
F(2A)-F(2B)-F(3A)-F(4B)	36(2)
B(1)-F(2B)-F(3A)-F(4B)	40.2(6)
F(2B)-B(1)-F(3B)-F(2A)	-6.0(8)
F(4B)-B(1)-F(3B)-F(2A)	-123.6(7)
F(4A)-B(1)-F(3B)-F(2A)	-132.8(6)
F(1)-B(1)-F(3B)-F(2A)	114.0(4)
F(3A)-B(1)-F(3B)-F(2A)	-69(2)
F(2B)-B(1)-F(3B)-F(4A)	126.8(7)
F(4B)-B(1)-F(3B)-F(4A)	9.2(8)
F(2A)-B(1)-F(3B)-F(4A)	132.8(6)
F(1)-B(1)-F(3B)-F(4A)	-113.3(4)
F(3A)-B(1)-F(3B)-F(4A)	64(3)
F(2B)-F(2A)-F(3B)-B(1)	13.6(17)
F(2B)-F(2A)-F(3B)-F(4A)	-19.8(19)
B(1)-F(2A)-F(3B)-F(4A)	-33.5(4)
F(2B)-B(1)-F(4A)-F(4B)	78(2)
F(2A)-B(1)-F(4A)-F(4B)	113.3(11)
F(1)-B(1)-F(4A)-F(4B)	-113.0(10)
F(3A)-B(1)-F(4A)-F(4B)	-3.0(11)
F(3B)-B(1)-F(4A)-F(4B)	163.3(13)
F(2B)-B(1)-F(4A)-F(3B)	-85.5(19)
F(4B)-B(1)-F(4A)-F(3B)	-163.3(13)
F(2A)-B(1)-F(4A)-F(3B)	-50.0(7)
F(1)-B(1)-F(4A)-F(3B)	83.6(7)
F(3A)-B(1)-F(4A)-F(3B)	-166.3(7)
B(1)-F(3B)-F(4A)-F(4B)	-20.4(16)
F(2A)-F(3B)-F(4A)-F(4B)	14.1(18)
F(2A)-F(3B)-F(4A)-B(1)	34.5(4)
F(3B)-F(4A)-F(4B)-B(1)	18.7(14)
B(1)-F(4A)-F(4B)-F(3A)	3.9(14)
F(3B)-F(4A)-F(4B)-F(3A)	23(3)
F(2B)-B(1)-F(4B)-F(4A)	-121.1(18)
F(2A)-B(1)-F(4B)-F(4A)	-87.1(16)
F(1)-B(1)-F(4B)-F(4A)	83.5(13)
F(3A)-B(1)-F(4B)-F(4A)	176.9(11)
F(3B)-B(1)-F(4B)-F(4A)	-16.1(12)
F(2B)-B(1)-F(4B)-F(3A)	62.0(15)
F(4A)-B(1)-F(4B)-F(3A)	-176.9(11)
F(2A)-B(1)-F(4B)-F(3A)	96.1(12)
F(1)-B(1)-F(4B)-F(3A)	-93.3(10)
F(3B)-B(1)-F(4B)-F(3A)	167.0(7)
B(1)-F(3A)-F(4B)-F(4A)	-4.4(16)
F(2B)-F(3A)-F(4B)-F(4A)	-42.0(19)
F(2B)-F(3A)-F(4B)-B(1)	-37.7(5)

Symmetry transformations used to generate equivalent atoms:
#1 -x+3/2,-y+1/2,-z+1

Datablock: I

```
Bond precision:      C-C = 0.0033 A              Wavelength=0.71073
Cell:        a=19.372(2)    b=12.2295(10)   c=11.3742(14)
             alpha=90       beta=124.421(8) gamma=90
Temperature: 291 K
                   Calculated                      Reported
Volume             2222.8(5)                       2222.8(5)
Space group        C 2/c                           C 2/c
Hall group         -C 2yc                          -C 2yc
Moiety formula     C18 H16 N4, 2(B F4), C2 N       C18 H16 N4, 2(B F4), C2 N
Sum formula        C20 H16 B2 F8 N5                C20 H16 B2 F8 N5
Mr                 500.00                          500.00
Dx,g cm-3          1.494                           1.494
Z                  4                               4
Mu (mm-1)          0.137                           0.137
F000               1012.0                          1012.0
F000'              1012.73
h,k,lmax           25,15,14                        24,15,14
Nref               2530                            2438
Tmin,Tmax          0.949,0.954
Tmin'              0.949
Correction method= Not given
Data completeness= 0.964       Theta(max)= 27.415
R(reflections)= 0.0617( 1793)      wR2(reflections)= 0.2111( 2438)
S = 1.132             Npar= 194
```

The following ALERTS were generated. Each ALERT has the format
test-name_ALERT_alert-type_alert-level.
Click on the hyperlinks for more details of the test.

Alert level C

PLAT029_ALERT_3_C _diffrn_measured_fraction_theta_full Low ..... 0.967 Note
PLAT234_ALERT_4_C Large Hirshfeld Difference F3B -- B1 .. 0.17 Ang.
PLAT244_ALERT_4_C Low 'Solvent' Ueq as Compared to Neighbors of B1 Check
PLAT244_ALERT_4_C Low 'Solvent' Ueq as Compared to Neighbors of C10 Check
PLAT761_ALERT_1_C CIF Contains no X-H Bonds ..... Please Check
PLAT762_ALERT_1_C CIF Contains no X-Y-H or H-Y-H Angles ..... Please Check

Alert level G

PLAT072_ALERT_2_G SHELXL First Parameter in WGHT Unusually Large. 0.13 Report
PLAT128_ALERT_4_G Alternate Setting for Input Space Group C2/c I2/a Note
PLAT302_ALERT_4_G Anion/Solvent Disorder ..... Percentage = 38 Note
PLAT304_ALERT_4_G Non-Integer Number of Atoms (1.50) in Resd. # 3 Check
PLAT344_ALERT_2_G Unusual sp? Angle Range in Solvent/Ion for . C11 Check
PLAT432_ALERT_2_G Short Inter X...Y Contact F2B .. C2 .. 2.91 Ang.
PLAT432_ALERT_2_G Short Inter X...Y Contact F2B .. C3 .. 2.94 Ang.
PLAT764_ALERT_4_G Overcomplete CIF Bond List Detected (Rep/Expd) . 1.27 Ratio
PLAT779_ALERT_4_G Suspect or Irrelevant (Bond) Angle in CIF .... # 22 Check
F4B -B1 -F4A 1.555 1.555 1.555 32.80 Deg.

PLAT779_ALERT_4_G Suspect or Irrelevant (Bond) Angle in CIF .... # 23
Check
F2B -B1 -F2A 1.555 1.555 1.555 31.20 Deg.

---

0 **ALERT level A** = Most likely a serious problem - resolve or explain
0 **ALERT level B** = A potentially serious problem, consider carefully
6 **ALERT level C** = Check. Ensure it is not caused by an omission or oversight
10 **ALERT level G** = General information/check it is not something unexpected

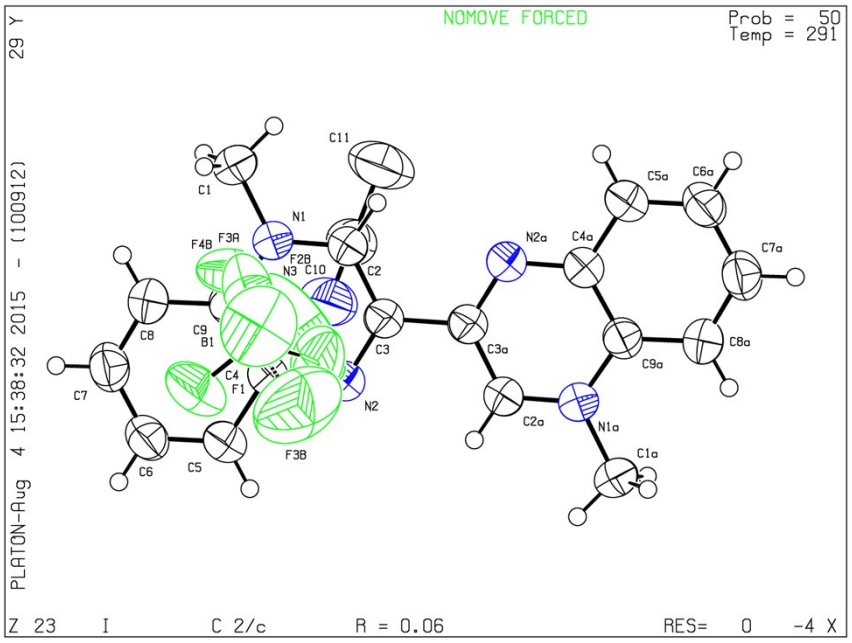

B_{12} - (Ebqn)$[BF_4]_2$

Table 1. Crystal data and structure refinement.

Empirical formula	C20 H20 B2 F8 N4
Formula weight	490.02
Temperature	180(2) K
Wavelength	0.71073 A
Crystal system, space group	Monoclinic, C 2/c
Unit cell dimensions	a = 9.371(4) A alpha = 90 deg. b = 14.361(7) A beta = 101.28(3) deg. c = 15.685(6) A gamma = 90 deg.
Volume	2069.9(15) A^3
Z, Calculated density	4, 1.572 Mg/m^3
Absorption coefficient	0.144 mm^-1
F(000)	1000
Crystal size	0.319 x 0.193 x 0.127 mm
Theta range for data collection	2.631 to 25.624 deg.
Limiting indices	-11<=h<=10, -17<=k<=17, -17<=l<=19
Reflections collected / unique	7293 / 1932 [R(int) = 0.0373]
Completeness to theta = 25.242	98.7 %
Absorption correction	None
Refinement method	Full-matrix least-squares on F^2
Data / restraints / parameters	1932 / 0 / 155
Goodness-of-fit on F^2	1.071
Final R indices [I>2sigma(I)]	R1 = 0.0389, wR2 = 0.0981
R indices (all data)	R1 = 0.0486, wR2 = 0.1082
Extinction coefficient	n/a
Largest diff. peak and hole	0.416 and -0.311 e.A^-3

Table 2. Atomic coordinates (x 10^4) and equivalent isotropic displacement parameters (A^2 x 10^3).
U(eq) is defined as one third of the trace of the orthogonalized Uij tensor.

	x	y	z	U(eq)
C(1)	5524(2)	1653(1)	6247(1)	33(1)
C(2)	8009(2)	1519(1)	7023(1)	30(1)
C(3)	9513(2)	1379(1)	7071(1)	29(1)
C(4)	9159(2)	1240(1)	5592(1)	29(1)
C(5)	9741(2)	1108(1)	4836(1)	33(1)
C(6)	8838(2)	1083(1)	4038(1)	36(1)
C(7)	7324(2)	1200(1)	3966(1)	35(1)
C(8)	6717(2)	1338(1)	4684(1)	32(1)
C(9)	7630(2)	1356(1)	5507(1)	28(1)
C(10)	4736(2)	733(1)	6234(1)	40(1)
N(1)	7108(1)	1507(1)	6262(1)	28(1)
N(2)	10083(2)	1252(1)	6378(1)	30(1)
F(1)	7929(2)	-552(1)	6796(1)	85(1)
F(2)	8326(1)	-2077(1)	6809(1)	57(1)
F(3)	6089(1)	-1544(1)	6864(1)	49(1)
F(4)	6938(2)	-1391(2)	5632(1)	89(1)
B(1)	7321(2)	-1397(1)	6520(1)	35(1)

Table 3. Bond lengths [A] and angles [deg].

C(1)-N(1)	1.495(2)
C(1)-C(10)	1.511(2)
C(2)-N(1)	1.320(2)
C(2)-C(3)	1.411(2)
C(3)-N(2)	1.315(2)
C(3)-C(3)#1	1.470(3)
C(4)-N(2)	1.360(2)
C(4)-C(5)	1.411(2)
C(4)-C(9)	1.423(2)
C(5)-C(6)	1.368(3)
C(6)-C(7)	1.411(3)
C(7)-C(8)	1.371(2)
C(8)-C(9)	1.402(2)
C(9)-N(1)	1.385(2)
F(1)-B(1)	1.374(3)
F(2)-B(1)	1.370(2)
F(3)-B(1)	1.383(2)
F(4)-B(1)	1.368(3)
N(1)-C(1)-C(10)	111.02(14)
N(1)-C(2)-C(3)	120.12(15)
N(2)-C(3)-C(2)	122.59(16)
N(2)-C(3)-C(3)#1	118.49(18)
C(2)-C(3)-C(3)#1	118.91(18)
N(2)-C(4)-C(5)	118.73(15)
N(2)-C(4)-C(9)	122.33(15)
C(5)-C(4)-C(9)	118.93(15)
C(6)-C(5)-C(4)	120.12(16)
C(5)-C(6)-C(7)	120.10(16)
C(8)-C(7)-C(6)	121.62(16)
C(7)-C(8)-C(9)	118.78(16)
N(1)-C(9)-C(8)	122.46(15)
N(1)-C(9)-C(4)	117.08(15)

C(8)-C(9)-C(4)	120.44(15)
C(2)-N(1)-C(9)	120.36(14)
C(2)-N(1)-C(1)	118.06(14)
C(9)-N(1)-C(1)	121.58(14)
C(3)-N(2)-C(4)	117.48(14)
F(4)-B(1)-F(2)	111.61(17)
F(4)-B(1)-F(1)	108.97(18)
F(2)-B(1)-F(1)	108.02(16)
F(4)-B(1)-F(3)	108.95(16)
F(2)-B(1)-F(3)	109.55(15)
F(1)-B(1)-F(3)	109.72(17)

Symmetry transformations used to generate equivalent atoms:
#1 -x+2,y,-z+3/2

Table 4. Anisotropic displacement parameters (A^2 x 10^3).
The anisotropic displacement factor exponent takes the form:
-2 pi^2 [h^2 a*^2 U11 + ... + 2 h k a* b* U12]

	U11	U22	U33	U23	U13	U12
C(1)	27(1)	35(1)	37(1)	-2(1)	6(1)	4(1)
C(2)	32(1)	27(1)	30(1)	-1(1)	6(1)	0(1)
C(3)	31(1)	26(1)	30(1)	1(1)	5(1)	-1(1)
C(4)	31(1)	25(1)	31(1)	1(1)	5(1)	-2(1)
C(5)	33(1)	34(1)	34(1)	1(1)	9(1)	-1(1)
C(6)	44(1)	34(1)	31(1)	0(1)	12(1)	-4(1)
C(7)	40(1)	32(1)	30(1)	1(1)	1(1)	-7(1)
C(8)	32(1)	29(1)	34(1)	2(1)	3(1)	-3(1)
C(9)	31(1)	23(1)	30(1)	1(1)	5(1)	-2(1)
C(10)	35(1)	42(1)	43(1)	0(1)	10(1)	-5(1)
N(1)	28(1)	25(1)	30(1)	0(1)	4(1)	0(1)
N(2)	30(1)	29(1)	31(1)	1(1)	5(1)	-1(1)
F(1)	66(1)	42(1)	143(2)	6(1)	6(1)	-7(1)
F(2)	41(1)	53(1)	80(1)	19(1)	17(1)	16(1)
F(3)	32(1)	74(1)	42(1)	4(1)	12(1)	5(1)
F(4)	48(1)	184(2)	36(1)	16(1)	11(1)	7(1)
B(1)	28(1)	43(1)	34(1)	9(1)	7(1)	4(1)

Table 5. Hydrogen coordinates (x 10^4) and isotropic displacement parameters (A^2 x 10^3).

	x	y	z	U(eq)
H(1A)	5100	2011	5736	39
H(1B)	5405	2005	6756	39
H(2)	7652	1620	7528	35
H(5)	10739	1039	4881	40
H(6)	9223	989	3541	43
H(7)	6723	1182	3419	42
H(8)	5718	1419	4626	39
H(1C)	5170	372	6732	59
H(10A)	4807	399	5714	59
H(10C)	3731	844	6247	59

Table 6. Torsion angles [deg].

N(1)-C(2)-C(3)-N(2)	1.4(2)
N(1)-C(2)-C(3)-C(3)#1	-178.89(10)
N(2)-C(4)-C(5)-C(6)	179.32(15)
C(9)-C(4)-C(5)-C(6)	-0.8(2)
C(4)-C(5)-C(6)-C(7)	0.8(2)
C(5)-C(6)-C(7)-C(8)	-0.1(3)
C(6)-C(7)-C(8)-C(9)	-0.5(2)
C(7)-C(8)-C(9)-N(1)	178.95(14)
C(7)-C(8)-C(9)-C(4)	0.5(2)
N(2)-C(4)-C(9)-N(1)	1.5(2)
C(5)-C(4)-C(9)-N(1)	-178.38(13)
N(2)-C(4)-C(9)-C(8)	-179.95(14)
C(5)-C(4)-C(9)-C(8)	0.2(2)
C(3)-C(2)-N(1)-C(9)	0.1(2)
C(3)-C(2)-N(1)-C(1)	179.61(14)
C(8)-C(9)-N(1)-C(2)	-179.92(14)
C(4)-C(9)-N(1)-C(2)	-1.4(2)
C(8)-C(9)-N(1)-C(1)	0.5(2)
C(4)-C(9)-N(1)-C(1)	179.07(13)
C(10)-C(1)-N(1)-C(2)	-95.52(17)
C(10)-C(1)-N(1)-C(9)	84.02(18)
C(2)-C(3)-N(2)-C(4)	-1.3(2)
C(3)#1-C(3)-N(2)-C(4)	178.99(9)
C(5)-C(4)-N(2)-C(3)	179.72(14)
C(9)-C(4)-N(2)-C(3)	-0.2(2)

Symmetry transformations used to generate equivalent atoms:
#1 -x+2,y,-z+3/2

Datablock: I

Bond precision: C-C = 0.0026 A Wavelength=0.71073
Cell: a=9.371(4) b=14.361(7) c=15.685(6)
alpha=90 beta=101.28(3) gamma=90
Temperature: 180 K

	Calculated	Reported
Volume	2070.1(16)	2069.9(15)
Space group	C 2/c	C 2/c
Hall group	-C 2yc	-C 2yc
Moiety formula	C20 H20 N4, 2(B F4)	C20 H20 N4, 2(B F4)
Sum formula	C20 H20 B2 F8 N4	C20 H20 B2 F8 N4
Mr	490.02	490.02
Dx,g cm-3	1.572	1.572
Z	4	4
Mu (mm-1)	0.144	0.144
F000	1000.0	1000.0
F000'	1000.73	
h,k,lmax	11,17,19	11,17,19
Nref	1968	1932
Tmin,Tmax	0.967,0.982	
Tmin'	0.955	

Correction method= Not given
Data completeness= 0.982 Theta(max)= 25.624
R(reflections)= 0.0389(1621) wR2(reflections)= 0.1082(1932)
S = 1.071 Npar= 155

The following ALERTS were generated. Each ALERT has the format
test-name_ALERT_alert-type_alert-level.
Click on the hyperlinks for more details of the test.

Alert level C

PLAT761_ALERT_1_C CIF Contains no X-H Bonds ..... Please Check
PLAT762_ALERT_1_C CIF Contains no X-Y-H or H-Y-H Angles ..... Please Check

Alert level G

PLAT244_ALERT_4_G Low 'Solvent' Ueq as Compared to Neighbors of B1 Check
PLAT790_ALERT_4_G Centre of Gravity not Within Unit Cell: Resd. # 2 Note
B F4

0 **ALERT level A** = Most likely a serious problem - resolve or explain
0 **ALERT level B** = A potentially serious problem, consider carefully
2 **ALERT level C** = Check. Ensure it is not caused by an omission or oversight
2 **ALERT level G** = General information/check it is not something unexpected

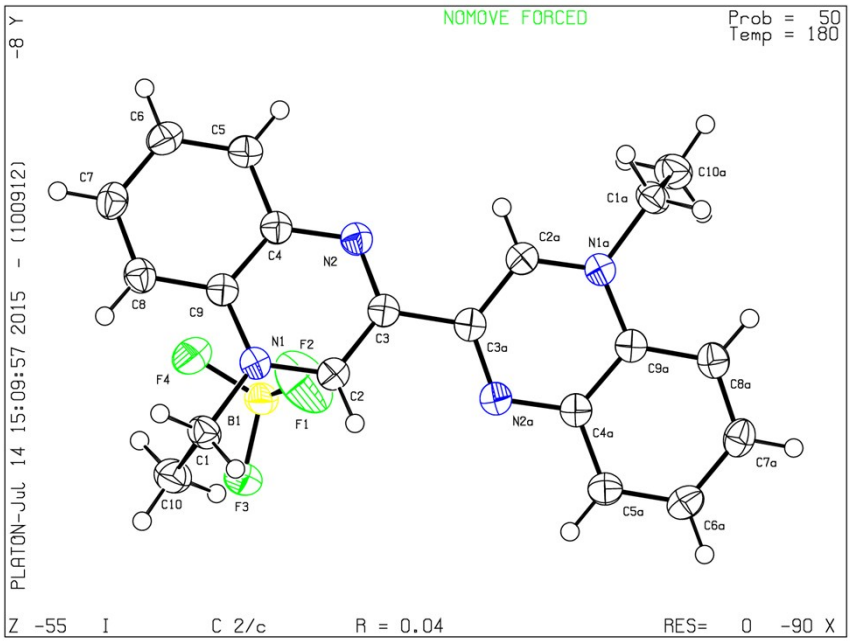

B_{14} -(Bzbqn)[BF_4]$_2$.2 MeCN

Table 1. Crystal data and structure refinement.

Empirical formula	C34 H30 B2 F8 N6
Formula weight	696.26
Temperature	291(2) K
Wavelength	0.71073 A
Crystal system, space group	Monoclinic, P 21/n
Unit cell dimensions	a = 8.6630(10) A alpha = 90 deg. b = 8.7810(10) A beta = 95.376(6) deg. c = 22.282(2) A gamma = 90 deg.
Volume	1687.5(3) A^3
Z, Calculated density	2, 1.370 Mg/m^3
Absorption coefficient	0.113 mm^-1
F(000)	716
Crystal size	0.341 x 0.316 x 0.309 mm
Theta range for data collection	2.452 to 27.389 deg.
Limiting indices	-11<=h<=11, -10<=k<=11, -24<=l<=28
Reflections collected / unique	7569 / 3732 [R(int) = 0.0258]
Completeness to theta = 25.242	97.9 %
Absorption correction	None
Refinement method	Full-matrix least-squares on F^2
Data / restraints / parameters	3732 / 0 / 275
Goodness-of-fit on F^2	1.071
Final R indices [I>2sigma(I)]	R1 = 0.0595, wR2 = 0.1801
R indices (all data)	R1 = 0.0874, wR2 = 0.1985
Extinction coefficient	n/a
Largest diff. peak and hole	0.411 and -0.379 e.A^-3

Table 2. Atomic coordinates (x 10^4) and equivalent isotropic displacement parameters (A^2 x 10^3).
U(eq) is defined as one third of the trace of the orthogonalized Uij tensor.

	x	y	z	U(eq)
C(1)	1904(3)	956(2)	4263(1)	62(1)
C(2)	701(2)	3153(2)	4687(1)	60(1)
C(3)	665(2)	4710(2)	4848(1)	58(1)
C(4)	2984(2)	5112(2)	4470(1)	57(1)
C(5)	4197(2)	6116(3)	4357(1)	64(1)
C(6)	5487(3)	5564(3)	4128(1)	68(1)
C(7)	5635(3)	4016(3)	4011(1)	69(1)
C(8)	4481(2)	3005(3)	4109(1)	64(1)
C(9)	3132(2)	3546(2)	4330(1)	56(1)
C(10)	1804(2)	742(2)	3592(1)	59(1)
C(11)	587(3)	1328(3)	3223(1)	74(1)
C(12)	545(4)	1098(4)	2604(1)	96(1)
C(13)	1682(5)	302(4)	2363(1)	98(1)
C(14)	2869(4)	-298(4)	2725(1)	92(1)
C(15)	2942(3)	-94(3)	3339(1)	73(1)
C(16)	-929(6)	7197(5)	2745(2)	132(1)
C(17)	-882(4)	5933(4)	3165(2)	99(1)
B(1)	2678(3)	351(3)	5875(1)	71(1)
N(1)	1893(2)	2608(2)	4436(1)	56(1)
N(2)	1751(2)	5667(2)	4734(1)	59(1)
N(3)	-844(4)	4945(4)	3487(2)	127(1)
F(1)	3129(3)	245(5)	6457(1)	182(1)
F(2)	1542(3)	1412(3)	5774(1)	133(1)
F(3)	2062(3)	-968(2)	5666(2)	170(1)
F(4)	3918(2)	683(2)	5564(1)	101(1)

Table 3. Bond lengths [A] and angles [deg].

C(1)-C(10)	1.501(3)
C(1)-N(1)	1.501(2)
C(2)-N(1)	1.311(3)
C(2)-C(3)	1.415(3)
C(3)-N(2)	1.304(3)
C(3)-C(3)#1	1.479(4)
C(4)-N(2)	1.356(3)
C(4)-C(5)	1.413(3)
C(4)-C(9)	1.418(3)
C(5)-C(6)	1.361(3)
C(6)-C(7)	1.392(3)
C(7)-C(8)	1.370(3)
C(8)-C(9)	1.393(3)
C(9)-N(1)	1.390(3)
C(10)-C(11)	1.375(3)
C(10)-C(15)	1.390(3)
C(11)-C(12)	1.390(4)
C(12)-C(13)	1.360(5)
C(13)-C(14)	1.353(5)
C(14)-C(15)	1.376(4)
C(16)-C(17)	1.450(5)
C(17)-N(3)	1.124(4)
B(1)-F(1)	1.323(3)
B(1)-F(3)	1.341(3)
B(1)-F(2)	1.358(3)
B(1)-F(4)	1.364(3)
C(10)-C(1)-N(1)	112.06(16)
N(1)-C(2)-C(3)	119.91(19)
N(2)-C(3)-C(2)	122.61(19)
N(2)-C(3)-C(3)#1	118.3(2)
C(2)-C(3)-C(3)#1	119.0(2)
N(2)-C(4)-C(5)	118.82(18)
N(2)-C(4)-C(9)	122.32(17)
C(5)-C(4)-C(9)	118.80(19)
C(6)-C(5)-C(4)	119.7(2)
C(5)-C(6)-C(7)	120.8(2)
C(8)-C(7)-C(6)	121.4(2)
C(7)-C(8)-C(9)	119.0(2)
N(1)-C(9)-C(8)	122.98(18)
N(1)-C(9)-C(4)	116.73(17)
C(8)-C(9)-C(4)	120.28(18)
C(11)-C(10)-C(15)	119.2(2)
C(11)-C(10)-C(1)	121.2(2)
C(15)-C(10)-C(1)	119.56(19)
C(10)-C(11)-C(12)	119.1(3)
C(13)-C(12)-C(11)	120.9(3)
C(14)-C(13)-C(12)	120.2(3)
C(13)-C(14)-C(15)	120.3(3)
C(14)-C(15)-C(10)	120.3(3)
N(3)-C(17)-C(16)	179.4(4)
F(1)-B(1)-F(3)	110.6(3)
F(1)-B(1)-F(2)	110.8(3)
F(3)-B(1)-F(2)	106.1(2)
F(1)-B(1)-F(4)	109.8(2)
F(3)-B(1)-F(4)	108.3(3)
F(2)-B(1)-F(4)	111.2(2)
C(2)-N(1)-C(9)	120.51(16)
C(2)-N(1)-C(1)	119.12(17)
C(9)-N(1)-C(1)	120.37(17)
C(3)-N(2)-C(4)	117.72(17)

Symmetry transformations used to generate equivalent atoms:
#1 -x,-y+1,-z+1

Table 4. Anisotropic displacement parameters (A^2 x 10^3).
The anisotropic displacement factor exponent takes the form:
-2 pi^2 [h^2 a*^2 U11 + ... + 2 h k a* b* U12]

	U11	U22	U33	U23	U13	U12
C(1)	75(1)	52(1)	62(1)	-2(1)	13(1)	-3(1)
C(2)	65(1)	59(1)	57(1)	-3(1)	12(1)	-6(1)
C(3)	63(1)	59(1)	53(1)	-4(1)	9(1)	-3(1)
C(4)	62(1)	58(1)	53(1)	-1(1)	7(1)	-5(1)
C(5)	69(1)	59(1)	64(1)	-2(1)	9(1)	-8(1)
C(6)	63(1)	74(1)	67(1)	2(1)	6(1)	-12(1)
C(7)	59(1)	82(1)	67(1)	-6(1)	9(1)	-3(1)
C(8)	62(1)	66(1)	63(1)	-7(1)	7(1)	-1(1)
C(9)	61(1)	58(1)	49(1)	-1(1)	5(1)	-3(1)
C(10)	63(1)	51(1)	64(1)	-6(1)	10(1)	-6(1)
C(11)	71(1)	75(1)	76(1)	-4(1)	2(1)	-1(1)
C(12)	101(2)	104(2)	77(2)	3(2)	-18(2)	-11(2)
C(13)	120(2)	108(2)	66(2)	-17(2)	13(2)	-20(2)
C(14)	103(2)	94(2)	84(2)	-28(1)	30(2)	-10(2)
C(15)	73(1)	71(1)	76(1)	-12(1)	12(1)	2(1)
C(16)	154(3)	105(2)	145(3)	24(2)	51(3)	8(2)
C(17)	102(2)	89(2)	112(2)	-3(2)	37(2)	0(2)
B(1)	65(1)	72(2)	75(2)	6(1)	5(1)	-7(1)
N(1)	63(1)	53(1)	52(1)	-2(1)	9(1)	-4(1)
N(2)	64(1)	57(1)	58(1)	-3(1)	9(1)	-4(1)
N(3)	144(3)	111(2)	131(2)	18(2)	43(2)	11(2)
F(1)	106(2)	351(4)	87(1)	53(2)	8(1)	32(2)
F(2)	124(2)	132(2)	147(2)	34(1)	22(1)	49(1)
F(3)	127(2)	99(1)	294(3)	-49(2)	67(2)	-48(1)
F(4)	85(1)	124(1)	95(1)	1(1)	20(1)	-26(1)

Table 5. Hydrogen coordinates (x 10^4) and isotropic displacement parameters (A^2 x 10^3).

	x	y	z	U(eq)
H(16A)	106	7443	2657	199
H(16B)	-1386	8067	2920	199
H(16C)	-1538	6919	2379	199
H(1A)	2850(30)	560(30)	4459(11)	69(6)
H(1B)	990(30)	590(30)	4406(12)	75(7)
H(2)	-90(30)	2490(30)	4755(12)	75(7)
H(5)	4060(30)	7110(30)	4459(10)	65(6)
H(6)	6340(30)	6260(30)	4064(12)	85(7)
H(7)	6630(40)	3650(30)	3857(13)	94(8)
H(8)	4610(30)	1980(30)	4052(11)	73(6)
H(11)	-170(30)	1950(30)	3414(12)	87(8)
H(12)	-250(40)	1610(40)	2377(15)	106(9)
H(13)	1780(40)	260(40)	1963(17)	105(10)
H(14)	3710(40)	-1010(40)	2545(16)	120(11)
H(15)	3850(30)	-480(30)	3598(13)	80(7)

Table 6. Torsion angles [deg].

N(1)-C(2)-C(3)-N(2)	3.1(3)
N(1)-C(2)-C(3)-C(3)#1	-177.8(2)
N(2)-C(4)-C(5)-C(6)	176.01(18)
C(9)-C(4)-C(5)-C(6)	-1.2(3)
C(4)-C(5)-C(6)-C(7)	-1.0(3)
C(5)-C(6)-C(7)-C(8)	1.6(3)
C(6)-C(7)-C(8)-C(9)	0.0(3)
C(7)-C(8)-C(9)-N(1)	179.19(17)
C(7)-C(8)-C(9)-C(4)	-2.2(3)
N(2)-C(4)-C(9)-N(1)	4.4(3)
C(5)-C(4)-C(9)-N(1)	-178.52(16)
N(2)-C(4)-C(9)-C(8)	-174.30(17)
C(5)-C(4)-C(9)-C(8)	2.8(3)
N(1)-C(1)-C(10)-C(11)	-57.5(3)
N(1)-C(1)-C(10)-C(15)	124.0(2)
C(15)-C(10)-C(11)-C(12)	-1.4(3)
C(1)-C(10)-C(11)-C(12)	-179.9(2)
C(10)-C(11)-C(12)-C(13)	0.2(4)
C(11)-C(12)-C(13)-C(14)	0.8(5)
C(12)-C(13)-C(14)-C(15)	-0.6(5)
C(13)-C(14)-C(15)-C(10)	-0.6(4)
C(11)-C(10)-C(15)-C(14)	1.6(4)
C(1)-C(10)-C(15)-C(14)	-179.8(2)
C(3)-C(2)-N(1)-C(9)	0.5(3)
C(3)-C(2)-N(1)-C(1)	-179.43(17)
C(8)-C(9)-N(1)-C(2)	174.70(18)
C(4)-C(9)-N(1)-C(2)	-4.0(2)
C(8)-C(9)-N(1)-C(1)	-5.3(3)
C(4)-C(9)-N(1)-C(1)	175.98(16)
C(10)-C(1)-N(1)-C(2)	112.9(2)
C(10)-C(1)-N(1)-C(9)	-67.1(2)
C(2)-C(3)-N(2)-C(4)	-2.6(3)
C(3)#1-C(3)-N(2)-C(4)	178.2(2)
C(5)-C(4)-N(2)-C(3)	-178.20(17)
C(9)-C(4)-N(2)-C(3)	-1.1(3)

Symmetry transformations used to generate equivalent atoms:
#1 -x,-y+1,-z+1

Datablock: I

Bond precision: C-C = 0.0035 A Wavelength=0.71073
Cell: a=8.663(1) b=8.781(1) c=22.282(2)
alpha=90 beta=95.376(6) gamma=90
Temperature: 291 K

	Calculated	Reported
Volume	1687.5(3)	1687.5(3)
Space group	P 21/n	P 21/n
Hall group	-P 2yn	-P 2yn
Moiety formula	C30 H24 N4, 2(B F4), 2(C2 H3 N)	C30 H24 N4, 2(B F4), 2(C2 H3 N)
Sum formula	C34 H30 B2 F8 N6	C34 H30 B2 F8 N6
Mr	696.26	696.26
Dx,g cm-3	1.370	1.370
Z	2	2
Mu (mm-1)	0.113	0.113
F000	716.0	716.0
F000'	716.44	
h,k,lmax	11,11,28	11,11,28
Nref	3827	3732
Tmin,Tmax	0.962,0.966	
Tmin'	0.962	
Correction method=	Not given	

```
Data completeness= 0.975        Theta(max)= 27.389
R(reflections)= 0.0595( 2296)      wR2(reflections)= 0.1985( 3732)
S = 1.071              Npar= 275
```

The following ALERTS were generated. Each ALERT has the format
test-name_ALERT_alert-type_alert-level.
Click on the hyperlinks for more details of the test.

Alert level C

PLAT029_ALERT_3_C _diffrn_measured_fraction_theta_full Low ..... 0.979 Note
PLAT244_ALERT_4_C Low 'Solvent' Ueq as Compared to Neighbors of C17 Check
PLAT761_ALERT_1_C CIF Contains no X-H Bonds ..... Please Check
PLAT762_ALERT_1_C CIF Contains no X-Y-H or H-Y-H Angles ..... Please Check

Alert level G

PLAT072_ALERT_2_G SHELXL First Parameter in WGHT Unusually Large. 0.12 Report
PLAT244_ALERT_4_G Low 'Solvent' Ueq as Compared to Neighbors of B1 Check
PLAT432_ALERT_2_G Short Inter X...Y Contact F2 .. C2 .. 2.90 Ang.

0 **ALERT level A** = Most likely a serious problem - resolve or explain
0 **ALERT level B** = A potentially serious problem, consider carefully
4 **ALERT level C** = Check. Ensure it is not caused by an omission or oversight
3 **ALERT level G** = General information/check it is not something unexpected

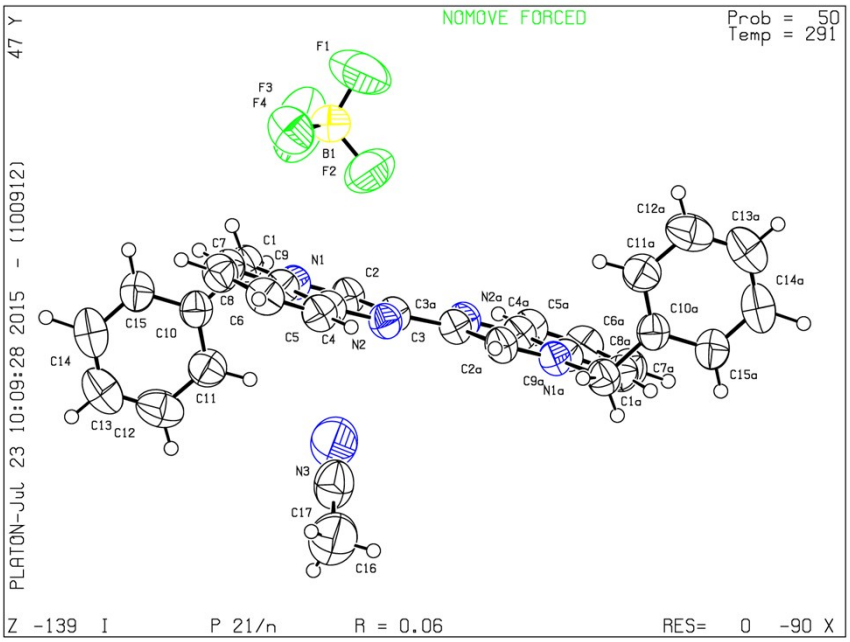

C. Additional characterisations

C_1 – Single crystal X-Ray structure of $[Pbqn^0\text{-}H^+]_2(S_4O_6^{2-})$

Empirical formula	2(C22 H25 N4), O6 S4
Formula weight	915.16
Temperature	150(2) K
Wavelength	1.54184 A
Crystal system, space group	Triclinic, P -1

Unit cell dimensions	a = 13.375(2) A alpha = 67.600(16) deg. b = 13.596(2) A beta = 70.371(15) deg. c = 13.843(2) A gamma = 69.377(15) deg.
Volume	2118.2(6) A^3
Z, Calculated density	2, 1.435 Mg/m^3
Absorption coefficient	2.557 mm^-1
F(000)	964
Crystal size	0.070 x 0.060 x 0.050 mm
Theta range for data collection	3.551 to 37.290 deg.
Limiting indices	-10<=h<=10, -10<=k<=10, -10<=l<=10
Reflections collected / unique	5154 / 2076 [R(int) = 0.0247]
Completeness to theta = 37.290	96.6 %
Absorption correction	Semi-empirical from equivalents
Max. and min. transmission	1.00000 and 0.78270
Refinement method	Full-matrix least-squares on F^2
Data / restraints / parameters	2076 / 0 / 304
Goodness-of-fit on F^2	1.072
Final R indices [I>2sigma(I)]	R1 = 0.0541, wR2 = 0.1321
R indices (all data)	R1 = 0.0593, wR2 = 0.1365
Extinction coefficient	0.0022(2)
Largest diff. peak and hole	0.544 and -0.413 e.A^-3

Table 2. Atomic coordinates (x 10^4) and equivalent isotropic displacement parameters (A^2 x 10^3) for pbqni.
U(eq) is defined as one third of the trace of the orthogonalized Uij tensor.

	x	y	z	U(eq)
C(1)	-6008(6)	-1491(6)	6006(5)	32(2)
C(2)	-6193(6)	-1042(5)	6923(5)	23(2)
C(3)	-5869(6)	38(5)	6497(5)	20(2)
C(4)	-5086(6)	357(5)	7668(5)	18(2)
C(5)	-5115(5)	820(5)	8395(5)	13(2)
C(6)	-7063(5)	1616(5)	8533(5)	14(2)
C(7)	-8043(5)	2252(5)	8958(5)	17(2)
C(8)	-8991(6)	2378(5)	8679(5)	20(2)
C(9)	-8953(6)	1873(5)	7977(5)	18(2)
C(10)	-7977(5)	1241(5)	7535(5)	18(2)
C(11)	-7012(5)	1110(5)	7798(5)	14(2)
C(12)	640(6)	-719(6)	6854(6)	42(2)
C(13)	-511(5)	-35(6)	7179(5)	27(2)
C(14)	-1173(5)	-693(5)	8186(5)	18(2)
C(15)	-3135(6)	66(5)	8350(5)	18(2)
C(16)	-4155(5)	738(5)	8700(5)	14(2)
C(17)	-3352(6)	1320(5)	9550(5)	15(2)
C(18)	-3434(6)	2006(5)	10123(5)	21(2)
C(19)	-2517(6)	2053(6)	10329(5)	23(2)
C(20)	-1500(6)	1395(5)	9985(5)	25(2)
C(21)	-1389(6)	709(6)	9429(5)	23(2)
C(22)	-2311(5)	668(5)	9193(5)	13(2)
C(23)	949(6)	6341(6)	9131(6)	32(2)
C(24)	1028(6)	5512(5)	8601(5)	25(2)
C(25)	785(6)	6115(5)	7503(5)	21(2)
C(26)	-67(6)	5123(5)	6997(5)	17(2)
C(27)	-50(5)	4417(5)	6500(5)	15(2)
C(28)	1902(5)	4096(5)	5899(5)	12(2)
C(29)	2898(5)	3531(5)	5401(5)	20(2)
C(30)	3863(6)	3676(6)	5408(5)	25(2)
C(31)	3845(6)	4386(5)	5902(5)	22(2)
C(32)	2865(6)	4944(5)	6410(5)	20(2)
C(33)	1878(5)	4809(5)	6418(5)	13(2)
C(34)	-5719(6)	5746(6)	8304(6)	43(2)
C(35)	-4700(5)	5368(6)	7493(5)	25(2)
C(36)	-3901(5)	4379(5)	8061(5)	22(2)
C(37)	-2002(5)	4394(5)	7234(5)	17(2)
C(38)	-995(6)	4112(5)	6559(5)	16(2)
C(39)	-1696(5)	3120(5)	6007(5)	12(2)
C(40)	-1549(6)	2466(5)	5379(5)	18(2)
C(41)	-2402(6)	2099(5)	5420(5)	22(2)
C(42)	-3409(6)	2376(5)	6089(5)	20(2)
C(43)	-3590(6)	3013(5)	6723(5)	19(2)
C(44)	-2728(5)	3396(5)	6680(5)	12(2)
N(1)	-5989(4)	506(4)	7336(4)	17(2)
N(2)	-6091(4)	1472(4)	8807(4)	18(2)
N(3)	-2241(4)	12(4)	8598(4)	14(2)
N(4)	-4289(4)	1349(4)	9321(4)	16(2)
N(5)	852(4)	5361(4)	6936(4)	16(2)
N(6)	918(4)	3973(4)	5893(4)	18(2)
N(7)	-2849(4)	4040(4)	7324(4)	16(2)
N(8)	-814(4)	3457(4)	5942(4)	17(2)
O(1)	-2725(4)	9522(4)	6100(4)	49(2)
O(2)	-1829(4)	8393(4)	4889(4)	52(2)
O(3)	-1096(5)	8106(5)	6372(4)	61(2)
O(4)	-2579(5)	5401(5)	9161(4)	60(2)
O(5)	-1688(5)	6737(5)	8938(4)	66(2)
O(6)	-3383(4)	6597(4)	10308(5)	48(2)
S(1)	-2027(2)	8484(2)	5943(2)	34(1)
S(2)	-3008(2)	7325(2)	6856(2)	43(1)
S(3)	-2709(2)	6450(2)	9260(2)	49(1)
S(4)	-3708(2)	7607(2)	8259(2)	55(1)

Table 3. Bond lengths [A] and angles [deg] for pbqni.

C(1)-C(2)	1.522(8)
C(2)-C(3)	1.520(8)
C(3)-N(1)	1.465(7)
C(4)-N(1)	1.356(7)
C(4)-C(5)	1.360(8)
C(5)-N(2)	1.373(7)
C(5)-C(16)	1.437(8)
C(6)-C(7)	1.371(8)
C(6)-N(2)	1.402(7)
C(6)-C(11)	1.403(8)
C(7)-C(8)	1.383(8)
C(8)-C(9)	1.367(8)
C(9)-C(10)	1.376(8)
C(10)-C(11)	1.391(8)
C(11)-N(1)	1.405(7)
C(12)-C(13)	1.511(9)
C(13)-C(14)	1.518(9)
C(14)-N(3)	1.480(7)
C(15)-N(3)	1.322(7)
C(15)-C(16)	1.395(8)
C(16)-N(4)	1.342(7)
C(17)-N(4)	1.377(7)
C(17)-C(18)	1.395(8)
C(17)-C(22)	1.404(8)
C(18)-C(19)	1.376(8)
C(19)-C(20)	1.381(8)
C(20)-C(21)	1.363(8)
C(21)-C(22)	1.401(8)
C(22)-N(3)	1.390(7)
C(23)-C(24)	1.521(8)
C(24)-C(25)	1.511(9)
C(25)-N(5)	1.475(7)
C(26)-N(5)	1.347(7)
C(26)-C(27)	1.368(8)
C(27)-N(6)	1.361(7)
C(27)-C(38)	1.433(8)
C(28)-C(29)	1.380(8)
C(28)-N(6)	1.387(7)
C(28)-C(33)	1.398(8)
C(29)-C(30)	1.377(8)
C(30)-C(31)	1.370(8)
C(31)-C(32)	1.370(8)
C(32)-C(33)	1.390(8)
C(33)-N(5)	1.409(7)
C(34)-C(35)	1.517(9)
C(35)-C(36)	1.521(9)
C(36)-N(7)	1.474(7)
C(37)-N(7)	1.332(7)
C(37)-C(38)	1.378(8)
C(38)-N(8)	1.367(7)
C(39)-N(8)	1.375(7)
C(39)-C(40)	1.392(8)
C(39)-C(44)	1.397(8)
C(40)-C(41)	1.375(8)
C(41)-C(42)	1.372(8)
C(42)-C(43)	1.366(8)
C(43)-C(44)	1.399(8)
C(44)-N(7)	1.409(7)
O(1)-S(1)	1.443(5)
O(2)-S(1)	1.439(5)
O(3)-S(1)	1.407(6)
O(4)-S(3)	1.429(6)
O(5)-S(3)	1.431(6)
O(6)-S(3)	1.474(5)
S(1)-S(2)	2.151(3)
S(2)-S(4)	1.971(3)
S(3)-S(4)	2.070(3)

C(3)-C(2)-C(1)	110.6(5)

N(1)-C(3)-C(2)	113.9(5)
N(1)-C(4)-C(5)	122.6(6)
C(4)-C(5)-N(2)	119.1(6)
C(4)-C(5)-C(16)	123.5(6)
N(2)-C(5)-C(16)	117.2(6)
C(7)-C(6)-N(2)	121.1(6)
C(7)-C(6)-C(11)	120.3(6)
N(2)-C(6)-C(11)	118.5(6)
C(6)-C(7)-C(8)	120.1(6)
C(9)-C(8)-C(7)	120.1(7)
C(8)-C(9)-C(10)	120.7(7)
C(9)-C(10)-C(11)	120.1(7)
C(10)-C(11)-C(6)	118.7(6)
C(10)-C(11)-N(1)	122.1(6)
C(6)-C(11)-N(1)	119.2(6)
C(12)-C(13)-C(14)	111.5(6)
N(3)-C(14)-C(13)	111.7(5)
N(3)-C(15)-C(16)	121.7(6)
N(4)-C(16)-C(15)	122.0(6)
N(4)-C(16)-C(5)	116.7(6)
C(15)-C(16)-C(5)	121.3(6)
N(4)-C(17)-C(18)	118.4(6)
N(4)-C(17)-C(22)	123.0(6)
C(18)-C(17)-C(22)	118.5(6)
C(19)-C(18)-C(17)	120.9(7)
C(18)-C(19)-C(20)	119.9(7)
C(21)-C(20)-C(19)	120.8(7)
C(20)-C(21)-C(22)	120.1(7)
N(3)-C(22)-C(21)	122.6(6)
N(3)-C(22)-C(17)	117.7(6)
C(21)-C(22)-C(17)	119.7(6)
C(25)-C(24)-C(23)	109.5(5)
N(5)-C(25)-C(24)	112.6(5)
N(5)-C(26)-C(27)	122.0(6)
N(6)-C(27)-C(26)	119.1(6)
N(6)-C(27)-C(38)	116.5(6)
C(26)-C(27)-C(38)	124.5(6)
C(29)-C(28)-N(6)	121.3(6)
C(29)-C(28)-C(33)	119.7(6)
N(6)-C(28)-C(33)	119.0(6)
C(30)-C(29)-C(28)	120.2(7)
C(31)-C(30)-C(29)	120.4(7)
C(32)-C(31)-C(30)	120.1(7)
C(31)-C(32)-C(33)	120.6(7)
C(32)-C(33)-C(28)	118.9(6)
C(32)-C(33)-N(5)	122.5(6)
C(28)-C(33)-N(5)	118.6(6)
C(34)-C(35)-C(36)	110.4(6)
N(7)-C(36)-C(35)	112.9(5)
N(7)-C(37)-C(38)	121.8(6)
N(8)-C(38)-C(37)	121.8(6)
N(8)-C(38)-C(27)	115.1(6)
C(37)-C(38)-C(27)	123.0(6)
N(8)-C(39)-C(40)	118.3(6)
N(8)-C(39)-C(44)	123.0(6)
C(40)-C(39)-C(44)	118.7(6)
C(41)-C(40)-C(39)	120.7(6)
C(42)-C(41)-C(40)	119.7(7)
C(43)-C(42)-C(41)	121.6(7)
C(42)-C(43)-C(44)	118.9(6)
C(39)-C(44)-C(43)	120.3(6)
C(39)-C(44)-N(7)	117.5(6)
C(43)-C(44)-N(7)	122.1(6)
C(4)-N(1)-C(11)	119.4(6)
C(4)-N(1)-C(3)	118.9(5)
C(11)-N(1)-C(3)	121.7(5)
C(5)-N(2)-C(6)	121.0(6)
C(15)-N(3)-C(22)	119.3(6)
C(15)-N(3)-C(14)	119.7(5)
C(22)-N(3)-C(14)	120.9(5)
C(16)-N(4)-C(17)	116.2(5)
C(26)-N(5)-C(33)	119.6(5)
C(26)-N(5)-C(25)	119.6(5)

C(33)-N(5)-C(25)	120.6(5)
C(27)-N(6)-C(28)	120.9(6)
C(37)-N(7)-C(44)	119.3(5)
C(37)-N(7)-C(36)	118.7(5)
C(44)-N(7)-C(36)	122.0(5)
C(38)-N(8)-C(39)	116.5(5)
O(3)-S(1)-O(2)	115.6(3)
O(3)-S(1)-O(1)	112.9(4)
O(2)-S(1)-O(1)	115.2(3)
O(3)-S(1)-S(2)	106.6(3)
O(2)-S(1)-S(2)	99.6(2)
O(1)-S(1)-S(2)	104.9(2)
S(4)-S(2)-S(1)	106.25(13)
O(4)-S(3)-O(5)	112.6(4)
O(4)-S(3)-O(6)	113.7(3)
O(5)-S(3)-O(6)	113.7(3)
O(4)-S(3)-S(4)	107.0(3)
O(5)-S(3)-S(4)	108.3(3)
O(6)-S(3)-S(4)	100.4(2)
S(2)-S(4)-S(3)	104.34(14)

Symmetry transformations used to generate equivalent atoms:

CHECK CIF.

Datablock: shelx

Bond precision: C-C = 0.0102 A Wavelength=1.54184
Cell: a=13.375(2) b=13.596(2) c=13.843(2)
alpha=67.600(16) beta=70.371(15) gamma=69.377(15)
Temperature: 150 K

	Calculated	Reported
Volume	2118.2(6)	2118.2(6)
Space group	P -1	P -1
Hall group	-P 1	-P 1
Moiety formula	2(C22 H25 N4), O6 S4	2(C22 H25 N4), O6 S4
Sum formula	C44 H50 N8 O6 S4	C44 H50 N8 O6 S4
Mr	915.16	915.16
Dx,g cm-3	1.435	1.435
Z	2	2
Mu (mm-1)	2.557	2.557
F000	964.0	964.0
F000'	969.19	
h,k,lmax	10,10,10	10,10,10
Nref	2148	2076
Tmin,Tmax	0.836,0.880	0.783,1.000
Tmin'	0.836	

Correction method= # Reported T Limits: Tmin=0.783
Tmax=1.000 AbsCorr = MULTI-SCAN
Data completeness= 0.966 Theta(max)= 37.289
R(reflections)= 0.0541(1858) wR2(reflections)= 0.1365(2076)
S = 1.072 Npar= 304

The following ALERTS were generated. Each ALERT has the format
test-name_ALERT_alert-type_alert-level.
Click on the hyperlinks for more details of the test.

Alert level A
THETM01_ALERT_3_A The value of sine(theta_max)/wavelength is less than 0.550
Calculated sin(theta_max)/wavelength = 0.3929
PLAT201_ALERT_2_A Isotropic non-H Atoms in Main Residue(s) 52
Report

Alert level B
REFNR01_ALERT_3_B Ratio of reflections to parameters is < 8 for a
centrosymmetric structure
sine(theta)/lambda 0.3929
Proportion of unique data used 1.0000
Ratio reflections to parameters 6.8289
PLAT088_ALERT_3_B Poor Data / Parameter Ratio 6.83
Note

PLAT340_ALERT_3_B Low Bond Precision on C-C Bonds ..... 0.01024 Ang.

Alert level C

ABSTY02_ALERT_1_C An _exptl_absorpt_correction_type has been given without a literature citation. This should be contained in the _exptl_absorpt_process_details field. Absorption correction given as multi-scan

PLAT018_ALERT_1_C _diffrn_measured_fraction_theta_max .NE. *_full ! Check

PLAT214_ALERT_2_C Atom O2 (Anion/Solvent) ADP max/min Ratio 4.3 oblate

PLAT220_ALERT_2_C Non-Solvent Resd 1 C Ueq(max)/Ueq(min) Range 3.2 Ratio

PLAT220_ALERT_2_C Non-Solvent Resd 2 C Ueq(max)/Ueq(min) Range 3.6 Ratio

PLAT242_ALERT_2_C Low 'MainMol' Ueq as Compared to Neighbors of S1 Check

PLAT790_ALERT_4_C Centre of Gravity not Within Unit Cell: Resd. # 1 Note

C22 H25 N4

PLAT911_ALERT_3_C Missing # FCF Refl Between THmin & STh/L= 0.393 73 Report

---

Alert level G

PLAT007_ALERT_5_G Number of Unrefined Donor-H Atoms ..... 2 Report

PLAT083_ALERT_2_G SHELXL Second Parameter in WGHT Unusually Large 6.97 Why ?

PLAT790_ALERT_4_G Centre of Gravity not Within Unit Cell: Resd. # 3 Note

O6 S4

PLAT909_ALERT_3_G Percentage of Observed Data at Theta(Max) Still 89 % Note

PLAT978_ALERT_2_G Number C-C Bonds with Positive Residual Density. 1 Note

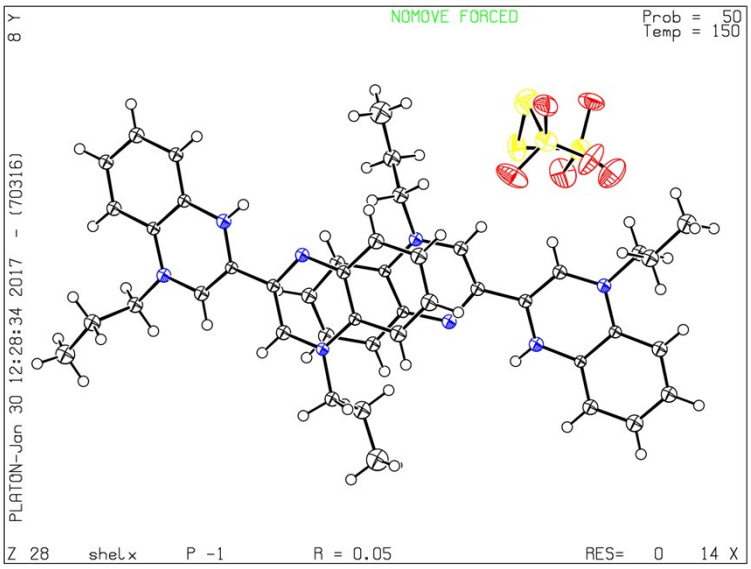

C_2 - Elemental Analysis on the intermediate purple powder made of R=Methyl, Ethyl, Propyl and Benzyl

The data are the experimental one.

Intermediate purple powder	%C	%H	%N	**%S**
R=Methyl	48.01	4.17	12.47	**11.4**
R=Ethyl	53.76	4.83	12.76	**6.98**
R=Propyl	53.20	5.29	11.31	
R=Benzyl	68.45	4.84	10.76	

C_3 – Solution state UV-Visible spectrum of $Ebqn(BF_4)_2$, $Pbqn(BF_4)_2$ and $Bzbqn(BF_4)_2$

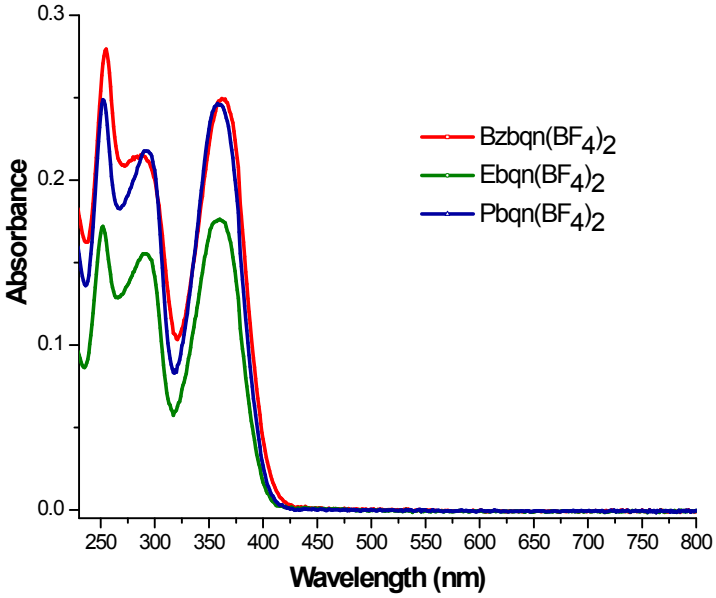

C_4 – Solid state infrared spectrum of $Ebqn(BF_4)_2$, $Pbqn(BF_4)_2$ and $Bzbqn(BF_4)_2$

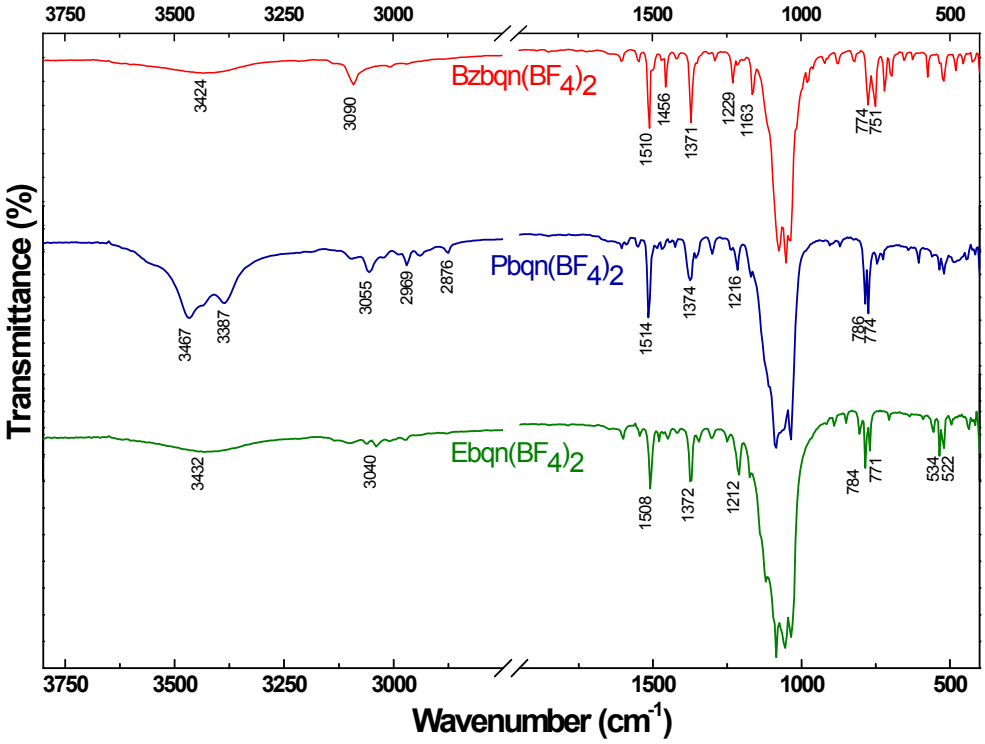

C_5 – Solid state UV-Visible spectrum of the intermediate reduced forms $Ebqn^0$-H^+, $Mbqn^0$-H^+, $Pbqn^0$-H^+ and $Bzbqn^0$-H^+

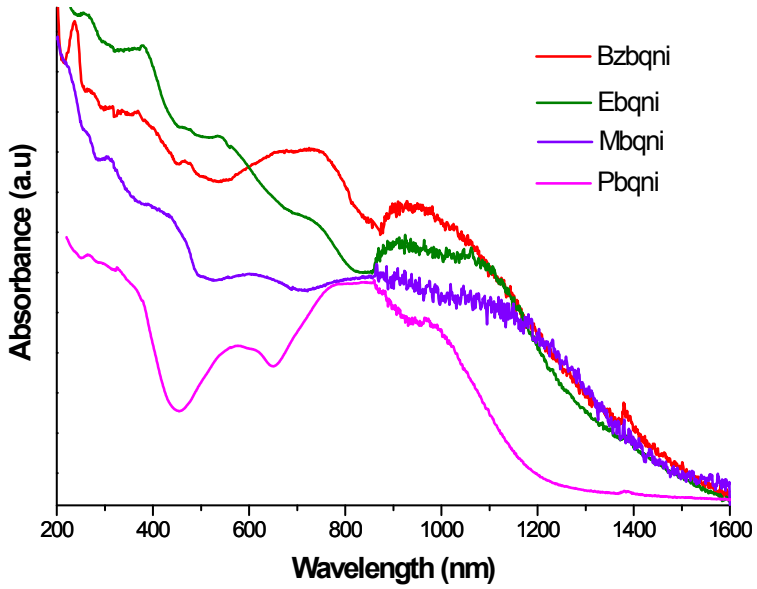

C_6 – Solid state infrared spectrum of the intermediate reduced forms Ebqn^0-H$^+$, Mbqn^0-H$^+$, Pbqn^0-H$^+$ and Bzbqn^0-H$^+$

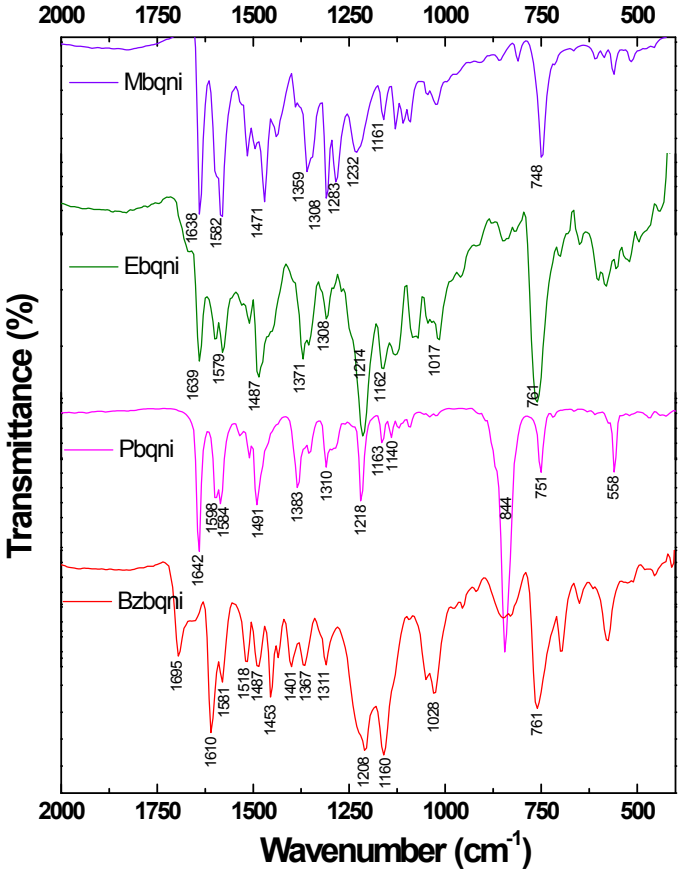

C_7 – DFT calculation on the *N*-methylquinoxalinium cation, radical and protonated radical cation (main geometrical parameters).

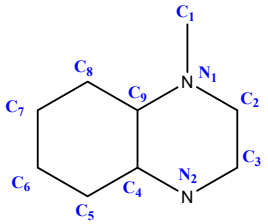

	N-methylquinoxalinium			
	Experimental	cation[a]	radical[a,b]	protonated radical cation[a,b]
C_1-N_1	1.479	1.481	1.458	1.465
C_9-N_1	1.370	1.382	1.395	1.398
C_8-C_9	1.385	1.405	1.398	1.398
C_7-C_8	1.361	1.377	1.393	1.387
C_6-C_7	1.363	1.413	1.395	1.397
C_5-C_6	1.341	1.370	1.387	1.385
C_5-C_4	1.402	1.415	1.407	1.395
C_4-C_9	1.389	1.435	1.430	1.418
C_4-N_2	1.357	1.350	1.376	1.383
N_2-C_3	1.295	1.314	1.347	1.356
N_1-C_2	1.305	1.332	1.376	1.365
C_2-C_3	1.393	1.401	1.370	1.361
Energy (hartree)		-457.502428589884	-457.726999544873	-458.190454548052

[a] All the values have been computed at the B3LYP/TZVP level of theory without symmetry restriction
[b] Solvation model using COSMO (ε=32,63, r=1.329)

C_8 – Additional EPR measurements

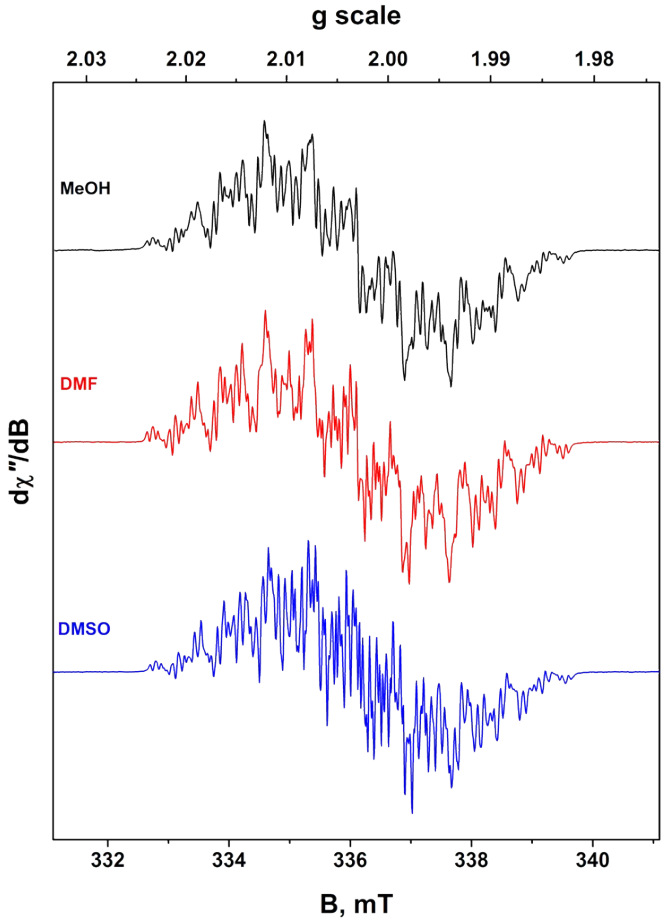

C8-1. Comparison of the radical formed from the reaction of *N*-methylquinoxalinium iodide and sodium dithionite in different solvents. Top: MeOH at 233 K; middle: DMF at 293 K; bottom: DMSO at 293 K.

This is the multiline spectrum indicative of *N*-methylquinoxalinyl radical, possibly protonated. The effect of tumbling as modulated by the solvent medium, gives a slightly sharper (narrower lines) profile in DMSO at ambient temperature. A chilled solution (-40 °C) is required for MeOH, though this was a more dilute solution. For the DMSO reaction, this spectrum was recorded 30 min after mixing; for the DMF reaction, this spectrum was recorded 48 h after initial mixing; for the MeOH reaction, this is a long-lived signal.

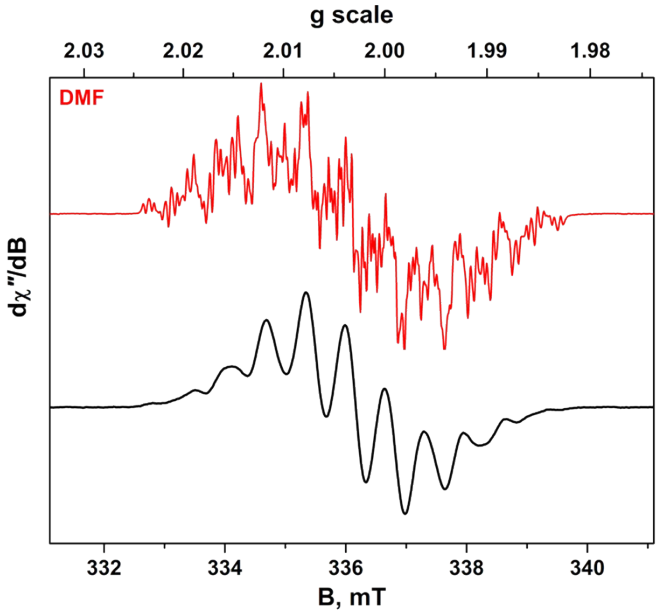

C8-2. Comparison of the radical formed from the reaction of *N*-methylquinoxalinium iodide and sodium dithionite in DMF after 24 h (red) and 72 h (black) at 293 K. The latter represents the spectrum for the $Mbqn^{\bullet+}$-H^+ radical,* here from coupling of two *N*-methylquinoxalinyl radicals formed initially.

The reaction progresses more slowly here than in the DMSO reaction (vide supra). A less concentrated sample was confined to a capillary tube where mixing was perturbed.

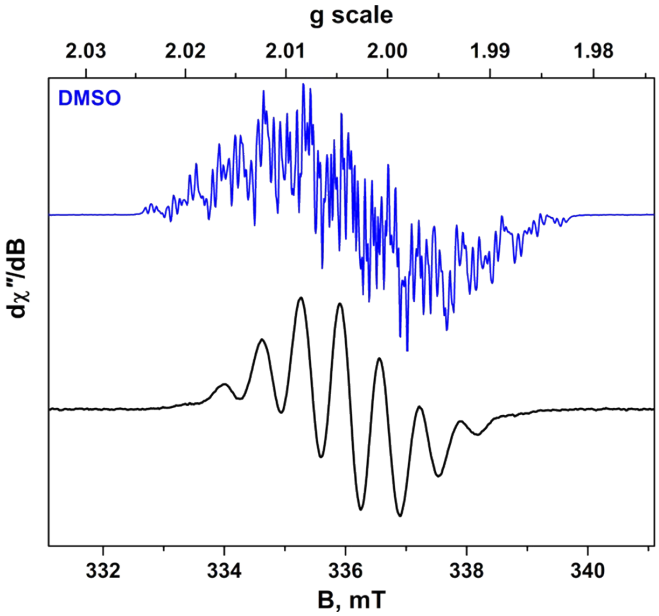

C8-3. Comparison of the radical formed from the reaction of *N*-methylquinoxalinium iodide and sodium dithionite in DMSO after 30 min (blue) and 24 h (black) at 293 K. The latter represents the spectrum for $Mbqn^{\bullet+}$-H^+ radical,* here from coupling of two *N*-methylquinoxalinyl radicals formed initially.

The reaction progresses much quicker in DMSO with a red colour quickly becoming dark purple to dark blue within a few hours.

* N. Leblanc, S. Sproules, K. Fink, L. Sanguinet, O. Aleveque, E. Levillain, P. Rosa and A. K. Powell, *Chem. Sci.*, 2016, **7**, 3820-3828.

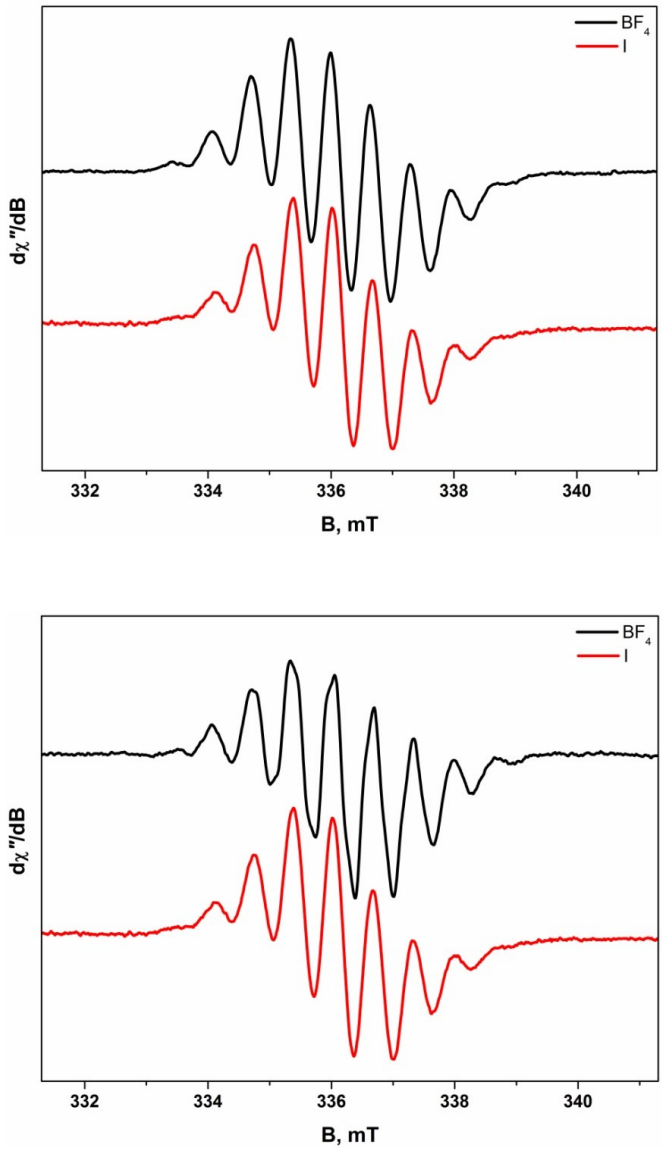

C8-4. Comparison of the X-band EPR spectra of the $Mbqn^{\bullet+}$-H^+ radical formed here *in situ* with BF_4^- (black) and I^- (red) counterions recorded in DMF solution at 233 K (top) and 293 K (bottom).

D. Experimental details

Single crystals X-Ray diffraction data of $[Mbqn](BF_4)_2$,MeCN, $[Ebqn](BF_4)_2$ and $[Bzqn](BF_4)_2$, 2 MeCN were collected at 180 K on a STOE IPDS II diffractometer equipped with a graphite monochromatized Mo Kα radiation (λ = 0.71073 Å), and mounted with an Oxford Nitrogen Cryostream. Data of $[Pbqn]_2$ (S_4O_6) have been collected at 150 K on an Agilent SuperNova diffractometer equipped with a Cu Kα x-ray source (λ = 1.54184 Å).

Structures were solved and refined using the Shelxl2013[†] and WingX2013[‡] packages and molecular diagrams were prepared using Diamond 4.2.2.[§] Positions, atomic displacement parameters, and hydrogens were refined by full-matrix least-squares routines against F^2.

EPR spectroscopy. X-band EPR spectra were recorded using a Bruker ELEXSYS E500 spectrometer and simulated using Bruker′s Xsophe software package.[**]

[†] G. Sheldrick, *Acta Cryst. A*, 2008, **64**, 112-122
[‡] L. Farrugia, *J. Appl. Cryst.*, 2012, **45**, 849-854
[§] H. Putz and K. Brandenburg, Diamond - Crystal and Molecular Structure Visualization, Kreuzherrenstr. 102, 53227 Bonn, Germany

Calculations. All calculations have been performed with the program package Orca 3.0.3.[††] In the DFT calculations[‡‡] the hybrid functional B3LYP[§§] in combination with the TZVP basis set[***] was used throughout. The influence of the MeOH solvent is considered by the conductor like screening model with a dielectric constant of 37.0.[†††] Artworks have been made with Chemissian[‡‡‡]

[**] Hanson, G. R. *et al.* XSophe-Sophe-XeprView®. A computer simulation software suite (v. 1.1.3) for the analysis of continuous wave EPR spectra. *Journal of Inorganic Biochemistry* **98,** 903-916 (2004).

[††] Neese, Frank (2012). "The ORCA program system". Wiley Interdisciplinary Reviews: Computational Molecular Science. 2 (**1**): 73–78.

[‡‡] O. Treutler and R. Ahlrichs, *J. Chem. Phys.*, 1995, **102**, 346-354.

[§§] (a) A.D. Becke, J.Chem.Phys. **98** (1993) 5648-5652. (b) C. Lee, W. Yang, R.G. Parr, Phys. Rev. B 37 (1988) 785-789.(c) S.H. Vosko, L. Wilk, M. Nusair, Can. J. Phys. 58 (1980) 1200-1211. (d) P.J. Stephens, F.J. Devlin, C.F. Chabalowski, M.J. Frisch, J.Phys.Chem. 98 (1994) 11623-11627.

[***] A. Schaefer, H. Horn, and R. Ahlrichs, "Fully optimized contracted Gaussian-basis sets for atoms Li to Kr," J. Chem. Phys., 97 (1992) 2571-77. A. Schaefer, C. Huber, and R. Ahlrichs, "Fully optimized contracted Gaussian-basis sets of triple zeta valence quality for atoms Li to Kr," J. Chem. Phys., 100 (1994) 5829-35.

[†††] (a) A. Klamt and G. Schuurmann, *J. Chem. Soc., Perkin Trans. 2*, 1993, 799-805; (b) A. Klamt, *The Journal of Physical Chemistry*, 1996, **100**, 3349-3353; (c) A. Klamt and V. Jonas, *J. Chem. Phys.*, 1996, **105**, 9972-9981.

[‡‡‡] http://www.chemissian.com/